Volume 48 | Number 6 | 21 March 2019 | Pages 1423–1854

Chem Soc Rev

Chemical Society Reviews
rsc.li/chem-soc-rev

Themed issue: Materials chemistry in flexible electronics

ISSN 0306-0012

ROYAL SOCIETY OF CHEMISTRY | Celebrating IYPT 2019

REVIEW ARTICLE
Yiran Yang and Wei Gao
Wearable and flexible electronics for continuous molecular monitoring

Chem Soc Rev

REVIEW ARTICLE

Cite this: *Chem. Soc. Rev.*, 2019, **48**, 1465

Wearable and flexible electronics for continuous molecular monitoring

Yiran Yang and Wei Gao *

Wearable biosensors have received tremendous attention over the past decade owing to their great potential in predictive analytics and treatment toward personalized medicine. Flexible electronics could serve as an ideal platform for personalized wearable devices because of their unique properties such as light weight, low cost, high flexibility and great conformability. Unlike most reported flexible sensors that mainly track physical activities and vital signs, the new generation of wearable and flexible chemical sensors enables real-time, continuous and fast detection of accessible biomarkers from the human body, and allows for the collection of large-scale information about the individual's dynamic health status at the molecular level. In this article, we review and highlight recent advances in wearable and flexible sensors toward continuous and non-invasive molecular analysis in sweat, tears, saliva, interstitial fluid, blood, wound exudate as well as exhaled breath. The flexible platforms, sensing mechanisms, and device and system configurations employed for continuous monitoring are summarized. We also discuss the key challenges and opportunities of the wearable and flexible chemical sensors that lie ahead.

Received 7th January 2018

DOI: 10.1039/c7cs00730b

rsc.li/chem-soc-rev

1. Introduction

The increasing research interest in personalized medicine – an innovative approach harnessing biomedical devices to deliver tailored diagnostics and therapeutics according to the individual characteristics of each patient – promises to revolutionize traditional medical practices.[1,2] This presents a tremendous opportunity for developing wearable devices toward predictive analytics and treatment. On the other hand, the Internet of Things (IoT) – sensors and actuators connected by networks – has received enormous attention in the past decade.[3,4] The IoT is expected to revolutionize future medicine by enabling highly personalized and accessible healthcare and will have an economic impact on the healthcare of over 1 trillion dollars in 2020.[3] As healthcare cost and the world's aging population increase, there has been a need for personalized wearable devices to continuously monitor the health status of patients while patients

Division of Engineering and Applied Science, California Institute of Technology, 1200 E California Blvd, Pasadena, CA 91125, USA. E-mail: weigao@caltech.edu

Yiran Yang

Yiran Yang received her BS degree in Bioengineering (magna cum laude) from Rice University. She then joined Dr Wei Gao's research group and is currently pursuing her PhD degree in Medical Engineering at Caltech. Her research interests include wearable electronics, biosensors and nanomedicine. She is also a member of the Tau Beta Pi Engineering Honor Society.

Wei Gao

Wei Gao is currently an Assistant Professor of Medical Engineering at the California Institute of Technology. He received his PhD in chemical engineering from the University of California, San Diego in 2014 (with Professor Joseph Wang) as a Jacobs Fellow and HHMI International Student Research Fellow. He worked as a postdoctoral fellow in Electrical Engineering and Computer Sciences at the University of California, Berkeley (with Professor Ali Javey) during 2014–2017. His current research interests include flexible electronics, wearable biosensors, micro/nanorobotics, and nanomedicine.

are out of hospital. In this case, wearable biosensors can sample physiological signals conveniently and noninvasively, and thus provide sufficient information for health monitoring and even preliminary medical diagnosis.[4–6]

Owing to their unique properties such as light weight, low cost, high flexibility, excellent stretchability, and great conformability, flexible electronics could serve as an ideal platform for personalized wearable devices.[7–17] Recent advances in the fabrication and development of flexible electronic devices coupled with novel micro/nanostructured materials have shown tremendous potential in a number of practical applications, including physiological monitoring, intelligent robotics, smart displays, and energy harvesting and storage.[18–28] In particular, wearable and flexible sensors have been demonstrated for tracking conventional physical signals in the past decade. These wearable devices are able to perform continuous physiological monitoring *via* real-time measurements of body motion, blood pressure, body and skin temperature, heart rate as well as electrophysiological activities including EEG (electroencephalography), ECG (electrocardiography) and EMG (electromyography).[29–42] Several key review articles on wearable and flexible electronic devices have been published in the past years with emphases on materials selection, sensor fabrication, device platforms, or their physical health monitoring applications.[43–48]

Despite the rapid growth in wearable and flexible sensing technologies, the commercially available wearable devices at present fail to provide more insightful information on users' health state at the molecular level. Biomarkers from the human body are defined as "molecules that can be objectively measured and evaluated as indicators of normal or disease processes and pharmacological responses to therapeutics" and can provide a dynamic and powerful access to understand a broad spectrum of health conditions, and will aid in the prediction, screening, diagnosis and therapy of diseases.[49,50] Biomarker monitoring has been used by generations of epidemiologists, physicians, engineers and scientists to study human diseases. However, many studies using biomarkers never achieve their full potential due to the lack of continuous monitoring technologies that could identify the roles of biomarkers in a timely manner. The instantaneous and continuous detection of relevant biomarkers in the human body using wearable chemical sensors can provide more in-depth personal healthcare monitoring and medical diagnosis, as compared to the detection of physical activities and vital signs. The limited availability of wearable chemical sensors has hindered further progress towards continuous personalized health monitoring. Up to now, there have been few single-platform, cost-effective, portable and fully-functional systems available in the market due to their respective inherent limitations.

2. Wearable and flexible chemical sensors

According to the International Union of Pure and Applied Chemistry (IUPAC), a chemical sensor is "a device that transforms chemical information, ranging from the concentration of a specific sample component to total composition analysis, into an analytically useful signal".[51] A typical chemical sensor usually consists of a recognition element (receptor) and a physicochemical transducer. The function of the receptor is to provide high selectivity towards the target analyte in the presence of potentially interfering chemicals while the transducer is the key component that converts the chemical information to a measurable analytical signal.

Wearable and flexible chemical sensors could be used as attractive alternatives to the bulky and expensive analytical instruments used in the healthcare sector. In traditional clinical settings, urine and blood samples are routinely analyzed through standard analytical techniques, which are expensive, time-consuming and unable to provide continuous measurements of the concentration of an analyte of interest. In addition, although the current gold-standard fluid for diagnostics is blood, it requires invasive sampling that poses a major hurdle and is unsuitable for long-term continuous use. Recognizing the significance of non-invasive wearable and flexible sensors for continuous molecular monitoring, researchers have focused tremendous effort on wearable and flexible techniques that can sample and analyze the major electrolytes, metabolites, heavy metals, and toxic gases directly in alternative body fluids, such as sweat, tears, interstitial fluid and saliva, as well as exhaustion breath, particularly in the past 5 years; researchers have also developed wearable epidermal sensors that can monitor wound healing (Fig. 1). The transition from blood to other body fluids and breath provides a noninvasive means of *in situ* sensing, which is more attractive toward continuous health monitoring in daily life. Based on the transduction technique, the wearable and flexible chemical sensors are mainly either electrochemical or optical in nature.

At present, electrochemical biosensing is the most common wearable and flexible sensing strategy owing to its unique advantages of sensor miniaturization, high sensitivity and label-free

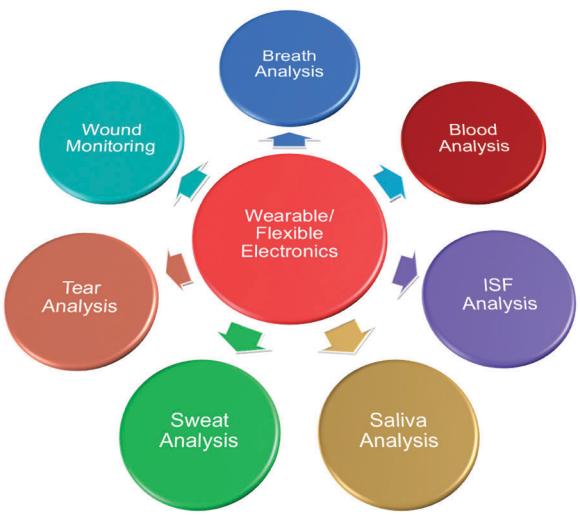

Fig. 1 Wearable and flexible chemical sensors for non-invasive health monitoring.

direct measurement.[52–56] Some classic examples of electrochemical sensors have been developed and demonstrated on wearable or flexible platforms over the years: (1) amperometric sensors. Amperometric sensors measure current generated from the oxidation or reduction of an electroactive analyte in a chemical reaction. Enzymatic amperometric sensors have been used for continuous monitoring of glucose, lactate, ethanol and uric acid, where chemical reactions of the target metabolite catalyzed by a specific enzyme (*e.g.* glucose oxidase, lactate oxidase and urate oxidase) generate electrical current proportional to the target concentration. (2) Potentiometric sensors. Potentiometry is usually defined as a zero-current technique that measures the potential appearing between the working electrode and the reference electrode in an electrochemical cell.[58] The ion selective electrode based potentiometric sensors have been widely used for selective ion quantification.[59] They usually contain a permselective membrane where the target ions interact with the corresponding ionophore (*e.g.* a sodium ionophore X for Na^+, valinomycin for K^+ and a calcium ionophore ETH 129 for Ca^{2+}) in the sensing membrane and cause voltage changes. For potentiometric sensors, the relationship between the analyte concentration and voltage output can be described by the Nernst equation: $E = RT/zF\cdot\ln(A/A_1) = \text{const} + S\cdot\log(A)$, where A and A_1 are ion activities/concentrations outside and inside the membrane, z is the charge of the ion, and S is the sensor sensitivity. For sodium or potassium sensing at room temperature, theoretically an ion selective sensor should have a sensitivity of 59.16 mV per decade of concentration. (3) Voltammetric sensors. Voltammetry is a very versatile and well-explored electroanalytical method and a transduction principle for deriving information about one or multiple analytes dynamically by measuring the current as a function of the varied potential. For example, stripping voltammetry is suitable for monitoring the heavy metals in body fluids.[58] (4) Electrochemical biosensors including affinity-based immunosensors and DNA sensors which have widely been used for analyzing proteins, peptides and DNAs/RNAs.

Optical sensing represents another attractive way for developing integrated chemical sensors owing to its low cost and simplicity.[60] Optical chemical sensors employ optical transduction techniques (*e.g.* colorimetric, fluorescence, and luminescence) to retrieve analyte information. The most widely used optical sensing technique in wearable and flexible electronics is colorimetry which refers to sensing elements undergoing a simple color change in the presence of a target analyte through a chemical reaction. Such a color change is typically quantified through a simple absorbance measurement where the sensing element is illuminated and the reflected or transmitted light is recorded. Specificity and sensitivity are typically dictated by the modified substrates or colorimetric chemical reactions. This technique has been explored for detecting metabolites (*e.g.* glucose and lactic acid) and electrolytes (*e.g.* H^+, Na^+ and Cl^-) in body fluids.[57]

When used for *in situ* analysis in physiological samples, wearable chemical sensors are subjected to many environmental effects that can affect their stability, reproducibility, and sensitivity. The challenges of on-body chemical analysis of body fluids and the early efforts of developing wearable chemical sensors for monitoring sweat have been summarized by Coyle *et al.* in previous reviews and book chapters.[52,61–63] In another review by Bandodkar and Wang, technological gaps impeding the successful realization of effective wearable chemical sensor systems were discussed, including material selection, power source and consumption, analytical procedure, wireless communication, data acquisition and processing, and protection of private information.[54] The emerging nanotechnology, materials science and flexible electronics have recently led to a remarkably rapid development in the field of wearable chemical and biochemical sensors, particularly in the past few years.[52–57]

This review focuses on the very recent advances of wearable and flexible electronics for non-invasive health monitoring through the *in situ* analysis of body fluids. In the following sections, we will mainly review separately the main research activities of continuous and non-invasive biomarker monitoring of human sweat, tears, saliva, blood, interstitial fluids, wound fluids as well as exhaled breath reported over the past few years. We will cover wearable and flexible substrates, conducting electrodes, sensing materials, device configurations and working principles employed for continuous biomarker monitoring. Finally, we will also discuss the overall challenges, opportunities and commercialization perspectives of wearable and flexible chemical sensors that lie ahead toward personalized health monitoring.

3. Wearable and flexible electronics for continuous molecular analysis

3.1. Sweat analysis

Sweat is a very important body fluid that contains rich information about our physiological state. The wide distribution of sweat glands in the human body and the abundant biochemical compounds in sweat have made sweat a feasible and ideal biofluid for non-invasive biosensing.[64–66] Eccrine sweat, which is easily accessible non-invasively, is excreted directly onto the surface of the skin and is composed of water and various electrolytes (*e.g.* sodium, potassium, calcium, and chloride), nitrogenous compounds (*e.g.* urea and amino acids), and metabolites such as glucose, lactate and uric acid. Xenobiotics such as drugs and ethanol can also be found in sweat.[67] Abnormal health conditions (*e.g.* electrolyte imbalance and physical stress) and diseases can alter sweat composition by either varying the concentration of common components or leading to the presence of new components. Sweat ethanol concentration is highly correlated with blood ethanol concentration; elevated sweat urea concentration is linked to kidney failure.[68–72] Abnormally high sweat chloride concentration is observed in cystic fibrosis (CF) patients and sweat chloride analysis has been adopted as the gold standard for cystic fibrosis diagnosis.[67,73,74] Despite many advantages, sweat analysis remains an underrepresented solution for health monitoring and clinical diagnosis compared to blood and urine analysis due to the challenges of contamination, evaporation as well as the lack of real time sweat sampling and sensing devices.

While sweat analysis has attracted tremendous attention in recent years, novel wearable and flexible sweat sensing platforms based on different detection approaches have been developed for *in situ* sweat analysis toward continuous health monitoring (Table 1 and Fig. 2). Specifically, sweat analytes are detected and quantified either with electrochemical and/or with optical methods on various flexible substrates such as textiles,[81,86,90–92,98] tattoo,[75–80] and plastic.[55,82,83,85,88,94,95,99,100] The electrochemical sweat sensors use functionalized electrodes to transduce sweat analyte concentration into electrical signals (*i.e.* current or voltage) which are transmitted to the processing component and give quantitative results with high sensitivity. The earliest-developed approach was based on a textile platform, which was used for sensing sweat pH, Na^+ levels, and sweat rate.[90–92] However, for most of the textile platforms tested *in situ*, the sensing results were severely affected by suboptimal contact between the sensor probe and human skin. In addition to textile-based platforms, a screen-printed tattoo-based sweat sensor was developed by Wang's group.[75–80] The tattoo platform was implemented through screen-printing technology on substrates such as silicone materials (*e.g.* PDMS, Ecoflex, Solaris) or polymer materials (*e.g.* PVA, PET, PEN). These materials have elastic properties similar to human skin and have enhanced the contact, adhesion and transpiration of the platform. Layers of electrode materials (such as carbon, Ag/AgCl) and insulators are printed on a tattoo paper sheet with designed patterns and the electrodes are then modified with sensing membranes. The temporary-transfer tattoo sweat biosensor is highly compact and flexible (Fig. 2a) and enables reliable continuous and *in situ* measurement of lactate, pH, Zn, ammonium and alcohol in sweat.[75–79] An adhesive radio-frequency identification (RFID) sensor bandage was reported which can chronologically monitor sweat sodium using an ion selective electrode based sodium sensor (Fig. 2b).[81] A commercial RIFD chip was adapted

Table 1 Wearable and flexible chemical sensors for continuous sweat analysis

Analyte	Analytical technique	Recognition element	Materials and platform	Ref.
Lactate	Electrochemical-amperometry	Lactate oxidase (LOx)	Temporary transfer tattoo	75
pH	Electrochemical-potentiometry	Polyaniline (PANI)	Temporary transfer tattoo	76
Zinc	Electrochemical-stripping voltammetry	Bismuth electrode	Temporary transfer tattoo	77
Ammonium	Electrochemical-potentiometry	Nonactin ionophore based ISE	Temporary transfer tattoo	78
Alcohol	Electrochemical-amperometry	Alcohol-oxidase	Temporary transfer tattoo	79
Sodium	Electrochemical-potentiometry	Sodium ionophore based ISE	Temporary transfer tattoo	80
Sodium	Electrochemical-potentiometry	Sodium ionophore based ISE	Textile-based bandage patch	81
Sodium, potassium, lactate, glucose	Electrochemical-potentiometry and amperometry	Sodium and potassium ISEs; glucose oxidase (GOx); LOx	PET wristband/handband	55
Ca, pH	Electrochemical-potentiometry	Calcium ISE; PANI	PET wristband/handband	82
Zn, Cd, Pb, Cu, Hg	Electrochemical-stripping voltammetry	Bismuth and gold electrodes	PET film	83
Humidity, glucose, pH	Resistive for humidity; electrochemical amperometry and potentiometry	PEDOT for humidity; GOx; polyaniline	Silicone wristband	56
Humidity, glucose, pH	Resistive for humidity; amperometry; potentiometry	PEDOT for humidity; GOx; PANI	Disposable silicone strip	84
pH	Electrochemical-transistor	ISFET for pH	PET patch	85
pH, metal ions	Optical-colorimetry	pH sensitive colorimetric indicators; Cu-sensitive and Fe-sensitive colorimetric indicators	Cellulose paper and silicone patch	86
pH	Optical-colorimetry	pH sensitive ionogels/dyes	Adhesive plaster/wristband	87
pH, lactate, chloride, glucose	Optical-colorimetry	LDH and diaphorase in formazan dyes; GOx with iodide; pH indicator dye; Hg^{2+} and Fe^{2+} with TPTZ	PDMS patch	57
Glucose, sodium, chloride	Electrochemical-potentiometry and amperometry	Sodium ISEs, Ag/AgCl electrode for chloride; glucose oxidase	PET wristband	88
Lactate, glucose	Electrochemical-amperometry	GOx; LOx	PDMS on a skin adhesive	89
pH	Optical-colorimetry	pH sensitive dye	Textile patch on a waistband	90
Sodium	Electrochemical-potentiometry	Sodium ionophore based ISE	Fabric patch on a belt	91
Sodium, pH	Electrochemical-impedance; optical-colorimetry	PPy based ISE; pH sensitive dyes	Fabric patch on a belt	92
EtG	Electrochemical-impedance	EtG antibody modified on ZnO or Au electrode	On either glass or polyimide	93
Chloride	Electrochemical-potentiometry	Ag/AgCl electrodes with salt bridge	PDMS on wristband or adhesive bandage	94
Sodium, chloride	Electrochemical-potentiometry	Sodium ISE, Ag/AgCl electrode	PET film attached to a memory foam and strap	95
Glucose, cortisol	Electrochemical-amperometry and impedance	Glucose oxidase on ZnO film; cortisol antibody on ZnO film	Polyamide film	96
Sodium	Electrochemical-potentiometry	Gold-nanodendrite ISE	Silicon chip on a flexible headband	97
Adrenaline, NaCl	Electrochemical-transistor	Pt for adrenaline, Ag gate for NaCl	Cotton wire	98
Lactate	Electrochemical-amperometry	Lactate oxidase	Polycarbonate membrane	99
Glucose, lactate, uric acid, urea	Piezoelectrical	LOx, GOx, uricase, and urease immobilized on ZnO nanowires	Kapton film	100
Potassium, lactate	Electrochemical-amperometry and potentiometry	LOx; potassium ISE	PET sticker on eyeglasses	101

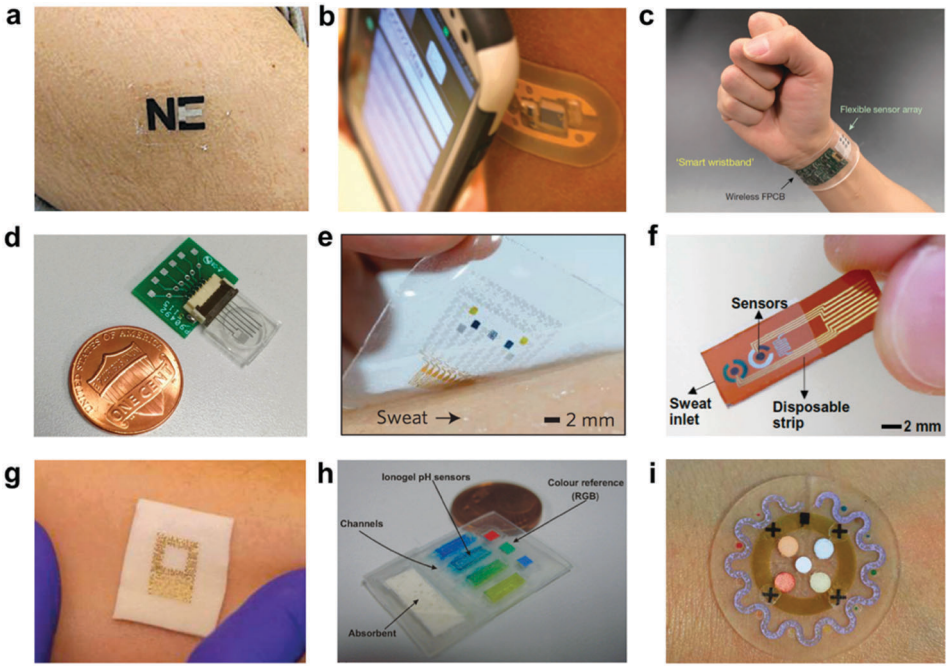

Fig. 2 Wearable and flexible sweat biosensors. (a) Epidermal temporary-transfer tattoo sweat biosensor for *in situ* continuous monitoring of lactate, pH, *etc.* Reproduced with permission from ref. 75. Copyright 2013 American Chemical Society. (b) Wireless sensor bandage for chronological monitoring of sweat Na^+ concentration. A RFID chip was incorporated for wireless communication with a smart phone. Reproduced with permission from ref. 81. Copyright 2015 IEEE. (c) Fully integrated "smart wristband" with a flexible sensor array and a flexible PCB for multiplexed *in situ* sweat analysis. Reproduced with permission from ref. 55. Copyright 2016 Nature Publishing Group. (d) Flexible sensor array for multiplexed heavy metal monitoring in sweat. Reproduced with permission from ref. 83. Copyright 2016 American Chemical Society. (e) Graphene-based flexible and stretchable diabetes patch for sweat glucose monitoring. Reproduced with permission from ref. 56. Copyright 2016 Nature Publishing Group. (f) A disposable strip for sweat glucose sensing. Reproduced with permission from ref. 84. Copyright 2017 American Association for the Advancement of Science. (g) Stretchable sensor with serpentine structure on porous polyurethane for sweat pH sensing. Reproduced with permission from ref. 86. Copyright 2014 Wiley. (h) Microfluidic-based device for sweat routing and colorimetric pH sensing. Reproduced with permission from ref. 87. Copyright 2012 Elsevier. (i) Stretchable microfluidic based sweat patch for spontaneous sweat routing through serpentine channels and the reservoir, with multiplexed colorimetric sensing. Reproduced with permission from ref. 57. Copyright 2016 American Association for the Advancement of Science.

to allow potentiometric sensing, temperature sensing and wireless communication with the smart phone.

Considering the complex correlation among all biophysical and biochemical information, simultaneous, accurate and multiplexed detection of the signatures with the capability of performing on-site data processing and communication is in urgent need. To this end, a fully integrated system was subsequently developed and widely applied in sweat sensing. Gao *et al.* merged plastic-based sensors that interface with the skin with integrated circuits consolidated on a flexible printed circuit board onto a flexible PET substrate, and achieved stable and accurate *in situ* monitoring of multiple sweat analytes including glucose, lactate, K^+ and Na^+ as well as skin temperature for signal calibration (Fig. 2c).[55] The integrated system takes the form of a smart wristband or headband and has stable contact with the skin; signal conditioning, processing and bluetooth based wireless transmission were consolidated in the flexible printed circuit board (FPCB) on the same wristband. The same group also developed a flexible microsensor array for heavy metal monitoring in sweat (Fig. 2d).[83] The ultra-low level multiplexed sweat heavy metal analysis was realized using gold and bismuth microelectrodes through anodic stripping voltammetry. The effective preconcentration step and selective oxidation of metal phase species make anodic stripping analysis the most effective technique for monitoring the ultralow levels of heavy metals in body fluids. The proposed wearable microsensor array was able to simultaneously detect Zn, Cd, Pb, Cu and Hg in human sweat during physical exercise. A graphene-based electrochemical sensor was developed by Lee *et al.* and applied for sweat glucose monitoring on a stretchable patch (Fig. 2e) and a disposable strip (Fig. 2f).[56,84] The device shows improved sensitivity and electrochemical activity due to the use of graphene-hybrid materials. The serpentine bilayer of gold mesh and gold-doped graphene formed an efficient electrochemical interface for the stable transfer of electrical signals. The large electrochemically active surface area of the graphene-hybrid electrode enabled the real time detection of low levels of sweat glucose (correlation factor between sweat and blood glucose in this work: $\sim$0.017). The reading from the glucose sensors was calibrated with real-time pH and temperature information obtained from pH and temperature sensors incorporated on the same platform to eliminate the influence of pH and temperature on the enzyme activity and on the glucose sensor response.

In addition to electrochemical sensors, wearable sensors based on optical methods were also developed on flexible platforms toward sweat analysis in recent years. For optical sweat sensing,

an optical fiber or digital camera was used to capture the colorimetric or absorbance response to color-responsive materials (*i.e.* pH dyes) of sensors, and quantitative results are generated by image analysis on a personal computer or a mobile phone. The optical detection method displays results to the wearer in real time and allows for simple interpretation of the analyte concentration. A stretchable sensor with a serpentine structure was fabricated on porous polyurethane and was used for pH measurements (Fig. 2g).[86] Another colorimetric sensor was developed on a microfluidic platform using a common reservoir to continuously draw sweat from the sensing area to four independent reservoirs housing ionogel pH dyes (Fig. 2h).[87] In addition to pH sensing, Koh *et al.* developed a stretchable microfluidic device that harvests and stores sweat from human skin, routes sweat to different channels with colorimetric assay reagents, and measures sweat rates as well as the levels of multiple sweat analytes including chloride, glucose, and lactate and pH (Fig. 2i).[57] The microfluidic network was designed to route sweat spontaneously through the network of serpentine channels and reservoirs. The reactions of the sensors with sweat analytes induce changes in the color of the chromogenic reagents. The integrated near field communication system between a sweat monitoring device and a smartphone enables image capture and analysis. The cellphone application can extract RGB color information and allow the user to read the sweat analyte concentrations.

The development of all the above-mentioned sweat sensors has opened the door of practical applications toward real-time monitoring of fitness and health conditions. The wearable and flexible sweat sensors have been tested intensively in human trials to extract more insightful information from sweat. For example, fully integrated wearable sensor arrays developed by Gao *et al.* have been used for effective and non-invasive identification of dehydration during long-term outdoor exercise (Fig. 3a).[55] Sweat Na^+ levels increased substantially when the subjects had lost a large amount of water (~2.5% of the body weight), indicating that sweat sodium can potentially serve as an important biomarker for monitoring dehydration. The wearable diabetes patch developed by Lee *et al.* can monitor the sweat glucose level electrochemically in real-time (sensing unit) and actuate transcutaneous diabetic drug release (therapeutic unit). Daily glucose monitoring *in vivo* was performed and changes in the sweat glucose concentration were well correlated with those of the blood glucose concentration (Fig. 3b).[56] Bioresorbable polymer-based micro-needles coated with the phase-change material were coupled with multichannel thermal actuators in the therapeutic unit such that the drug was released in a stepwise manner when the programmed temperature

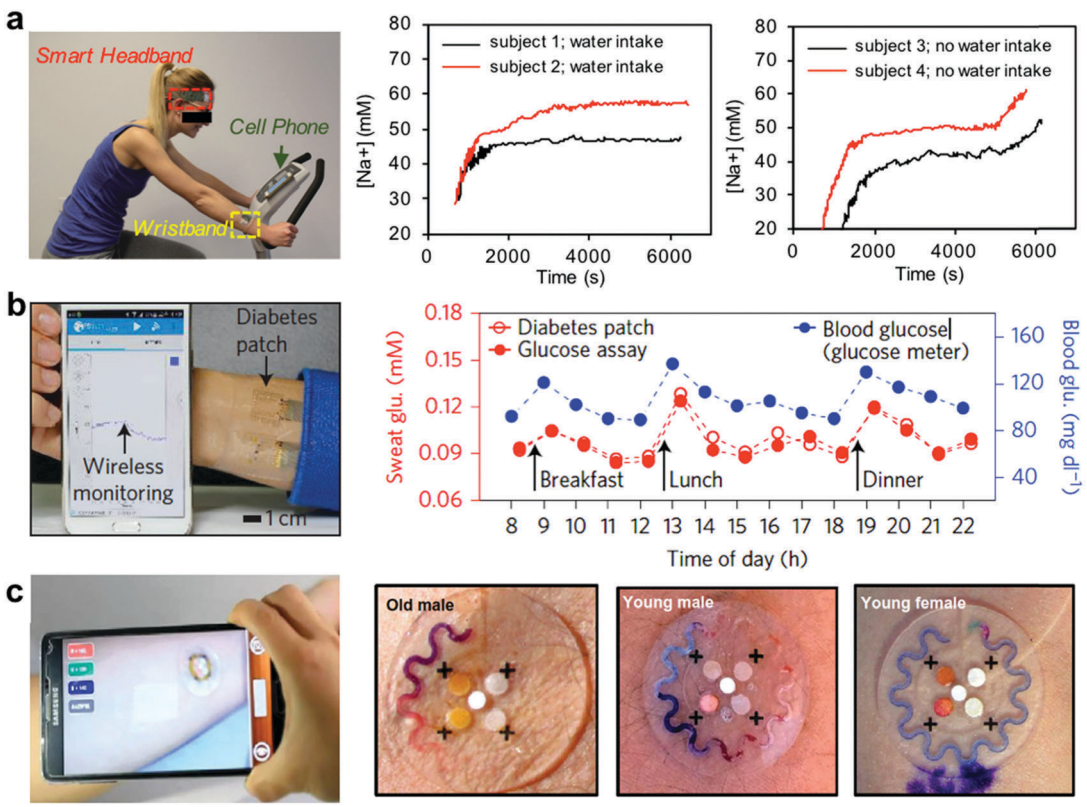

Fig. 3 Physiological and clinical investigations through human trials using wearable and flexible sweat biosensors. (a) Fully integrated headband and wristband for dehydration status monitoring during long-term exercise. Reproduced with permission from ref. 55. Copyright 2016 Nature Publishing Group. (b) Wearable diabetes patch for real-time monitoring of the daily sweat glucose level. Reproduced with permission from ref. 56. Copyright 2016 Nature Publishing Group. (c) Wearable optical sensor patch for real-time sweat rate monitoring of different subjects during a long-distance bicycling race. Reproduced with permission from ref. 57. Copyright 2016 American Association for the Advancement of Science.

exceeded the threshold as a response of glucose levels. The stretchable optical sweat sensor developed by Koh *et al.* was tested on human subjects in a competitive long-distance outdoor bicycling race (Fig. 3c).[57] The data showed that older subjects (aged 50 to 69 years) had greater sweat rates compared to younger subjects (aged 10 to 29 years), and male subjects exhibited larger sweat rates than females.

The *in situ* sweat sensor tests described above were mostly carried out with subjects performing vigorous exercise such as running or cycling to generate sweat. Although sweat production by exercising is viable for sensor testing, it might not be the ultimate solution for continuous sweat monitoring, particularly for sedentary individuals. In such cases, alternative methods of sweat induction are desired and need to be introduced. One well-developed sweat induction method is iontophoresis, which is widely used to induce sweat excretion locally as selected, usually on wrist. A charged substance, usually pilocarpine, is applied to the skin at one end of the test site. With the applied electrical potential difference between both ends of the test site, a mild electric current carries the pilocarpine into the skin and sweat glands are stimulated (Fig. 4a).[88,102] Based on this sweat induction approach, Kim *et al.* combined pilocarpine iontophoresis with *in situ* sweat alcohol sensing (Fig. 4b).[79]

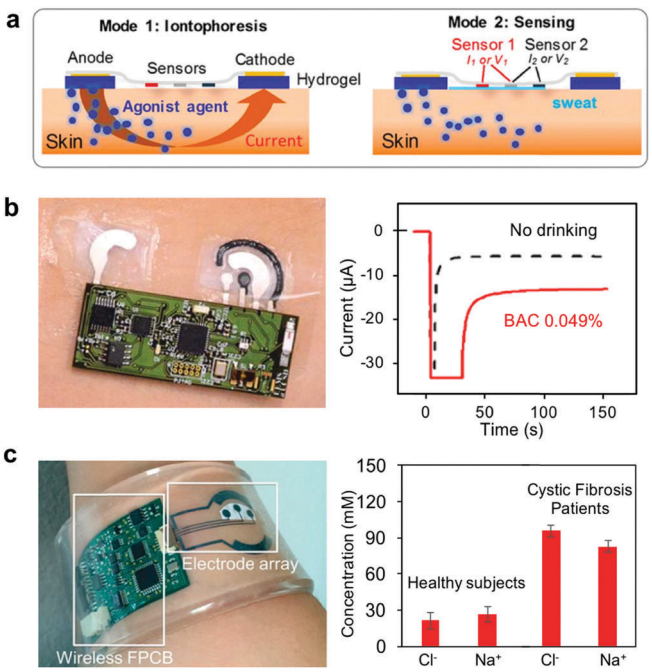

Fig. 4 Iontophoresis based sweat induction and sensing toward clinical applications. (a) Mechanism of iontophoresis in sweat sensing applications. Reproduced with permission from ref. 88. Copyright 2017 National Academy of Sciences USA. (b) Tattoo-based iontophoretic-biosensing system for sweat ethanol monitoring. A significantly increased current response of the wearable ethanol sensor was observed after alcohol intake. Reproduced with permission from ref. 79. Copyright 2016 American Chemical Society. (c) A fully integrated platform for controlled iontophoresis sweat induction and real-time sweat sensing. Real-time sensing results of sweat Na^+ and Cl^- levels distinguished cystic fibrosis patients from healthy subjects. Reproduced with permission from ref. 88. Copyright 2017 National Academy of Sciences USA.

By applying constant current through screen-printed "tattoo" AgCl iontophoresis electrodes, sweat was inducted and immediately used for sweat ethanol measurement by sensing electrodes; the sensing results can be transmitted wirelessly for data readout. The screen-printed "tattoo"-based ethanol sensing electrode relied on ethanol oxidase with the Prussian blue (PB) electrode transducer. With this sweat inducing and sensing device, on-body ethanol amperometric sensing yields a significant increase in current response after alcohol consumption (Fig. 4b), reflecting the good correlation between sweat and blood ethanol levels. Similarly, a fully integrated wearable sweat extraction and sensing platform was developed which contains a miniaturized iontophoresis module capable of inducing sweat with different excretion rate profiles and at periodic intervals (Fig. 4c).[88] The secretion rate pattern was controlled by controlling the compound formulation (*e.g.* acetylcholine, methacholine, and pilocarpine) loaded into iontophoresis hydrogels. The placement of the sensing electrodes between iontophoresis electrodes enables on-site analysis of induced sweat. The electrochemical electrodes were used to measure glucose, Na^+, and Cl^- with high sensitivity in sweat. With this device, diagnosis and disease investigation could be made. In this study, real-time Cl^- and Na^+ levels in sweat are much higher in CF patients than in healthy individuals (Fig. 4c). The device was also used to investigate the correlation between sweat and blood glucose levels. This fully autonomous sweat induction and analysis device leads to more potential sweat sensing applications such as point-of-care diagnosis and health monitoring.

The fast progress in sweat sensing platforms has expedited research on sweat sampling, as it is critical for improving the temporal resolution toward real-time sweat analysis and for minimizing the evaporation and contamination of the sweat samples. Peng *et al.* developed a new oil/membrane approach with the use of carbachol for sweat stimulation that could reduce the sample volume from the μL to nL regime and minimize analyte contamination (Fig. 5a).[103] By using a cosmetic-grade oil and a micro-porous membrane between skin and sensors, the sampling intervals are on the order of minutes, and the hydrophilic contaminants from the skin surface are blocked. Sonner *et al.* optimized the sensor geometry to improve the conduction of iontophoresis sweat flow.[94] Carbachol has shown prolonged sweat stimulation in directly stimulated regions for five hours or longer. Choi *et al.* developed a skin-like sweat sensor that collects and stores sweat in a set of interconnected micro-reservoirs (Fig. 5b).[104] The sweat sample was guided passively by the sweat gland induced pressure to a micro-channel network that incorporates capillary bursting valves in a sequential fashion and allows for chrono-monitoring. A soft wearable microfluidic system for measuring secretory fluidic pressures generated by eccrine sweat glands was also demonstrated by the same group.[105] The combination of iontophoresis and chrono-sampling microfluidics could possibly bring time-dependent sweat analysis in future applications. An epidermal microfluidic system was developed by Martín *et al.* for enhanced sweat sampling and metabolite detection (Fig. 5c).[89] Theoretical modeling of the microfluidic device design

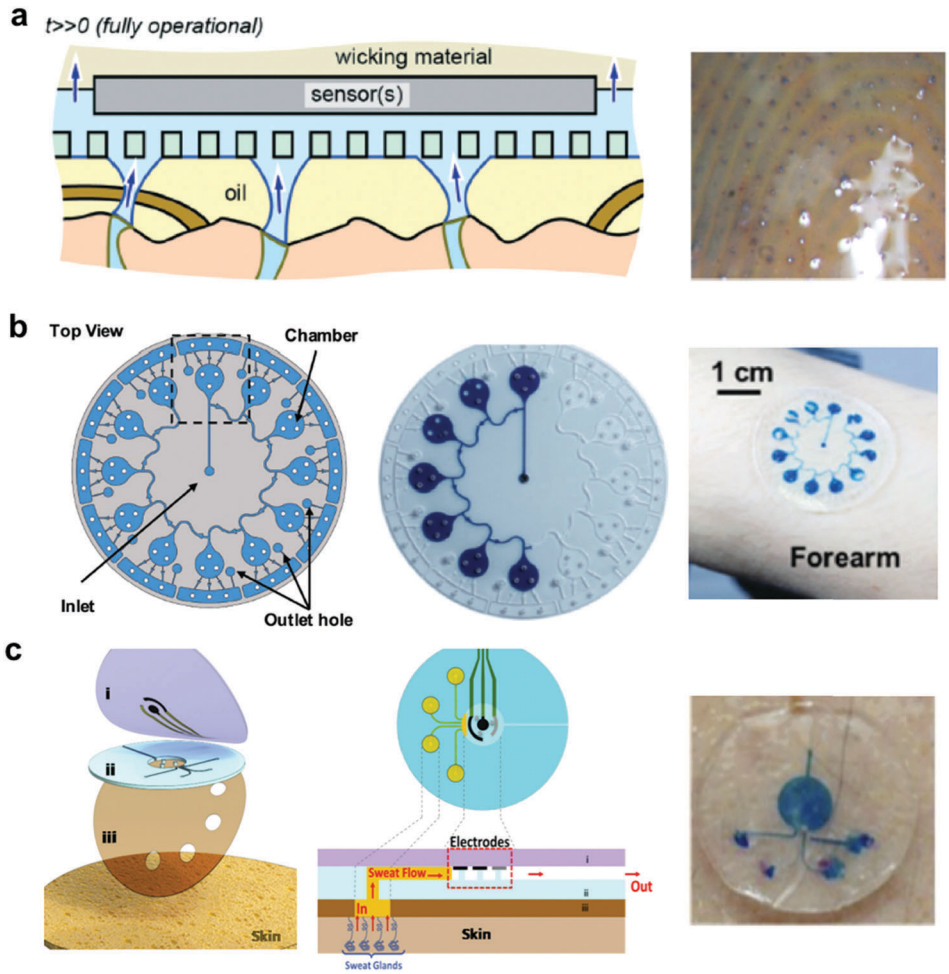

Fig. 5 New approaches for enhanced sweat sampling and sensing. (a) Oil-membrane approach with carbachol for sweat induction. A cosmetic-grade oil and a micro-porous membrane were used between skin and sensors. Reproduced with permission from ref. 103. Copyright 2016 Royal Society of Chemistry. (b) Micro-channel network based sweat sensor that collects and stores sweat in micro-reservoirs, allowing for chrono-monitoring of sweat analytes. Reproduced with permission from ref. 104. Copyright 2017 Wiley. (c) Epidermal three-layered microfluidic device with enhanced sweat sampling efficiency and transmission of sweat samples to sensing electrodes. Reproduced with permission from ref. 89. Copyright 2016 American Chemical Society.

allowed optimization of the sweat sampling process. This system enabled efficient sweat pumping to the electrochemical detection chamber containing the enzymatic glucose and lactate sensing electrodes.

Recent advances in sweat sensing application have proved sweat to be an excellent candidate for non-invasive continuous health monitoring. As more biomarkers are identified in sweat, it can be expected that sweat sensing would be expanded to more practical medical applications. Despite the non-invasive nature of sweat sensing, there are still major challenges to be addressed for continuous on-body sweat monitoring. Sweat can be generated in different ways (*e.g.* heat, exercise and iontophoresis) at different rates, and the levels of sweat biomarkers (*e.g.* glucose) could be much lower than those in blood. Sweat sensing at low sweat rates (*i.e.* in sedentary individuals) will require miniaturized sensors with higher sensitivity. Small volumes of sampled sweat would be susceptible to evaporation and contamination issues, which would lower the accuracy of the sensing results. To resolve these problems, *in situ* sampling of sweat should be carefully designed and fast detection is needed. Mixing of the newly sampled sweat and measured sweat samples can affect the real-time sensing results and lower the chrono-accuracy. Controlled sweat flow is necessary to improve the temporal resolution toward accurate real-time measurements. For some sweat analytes such as NaCl, their concentrations in sweat are sweat-rate dependent, so the measured results for these analytes should be calibrated with sweat rates. To expand the broad use of sweat-based medical or fitness monitoring, it is very critical to identify relevant analytes present in sweat and understand the physiological pathway of analyte secretion into sweat. Previous studies have shown that the excretion of sweat biomarkers can be different from each other (passive, active, or self-generating).[68] In particular, though some small molecules (*e.g.* Na, Cl, K, and Ca ions) could be theorized to passively or actively partition from blood, plasma or serum, up until now the excretion mechanisms of many sweat biomarkers (*e.g.* hormones, peptides or proteins)

have not been well understood as partitioning of these larger molecules may result from complex or varied pathways.

3.2. Tear analysis

The human tear is a biofluid accumulated in the eyes and it contains a number of salts, proteins, enzymes, and lipids. The chemical composition of tears can reveal useful information on ocular conditions and systemic disorders.[106,107] For example, the increased level of proline-rich protein 4 was identified as a biomarker for dry-eye conditions; modified expression of cancer-related biomarkers such as complement proteins was found in breast cancer patients; tear glucose concentration is highly correlated with blood glucose concentration and human tears have been used for continuous diabetes management.[108–110]

Earlier wearable and flexible tear glucose sensors were developed as flexible strips.[111–113] In the work of Kudo *et al.* (Fig. 6a), a flexible and stretchable glucose sensor was prepared on a flexible PDMS substrate and then coated by a hydrogen peroxide permeable poly(MPC-*co*-DMA) membrane.[111] The glucose sensor measures tear glucose concentration amperometrically with the use of glucose oxidase (GOx). In a later work from the same group, the tear glucose concentration was measured with GOx immobilized on a flexible oxygen electrode, and a gas permeable membrane was used. The device was tested *in vivo* on an anesthetized rabbit and the output current was monitored before and after oral glucose administration. The change in tear glucose was detected with 10–20 min delay compared to measured blood glucose change.[112] The strip-shaped sensor was difficult to fix on pupil due to insufficient contact area and flimsy movement, and Chu *et al.* improved this flexible strip structure by attaching the strip sensor to a contact lens (Fig. 6b).[113] In this case, the soft PDMS contact lens was molded; the flexible

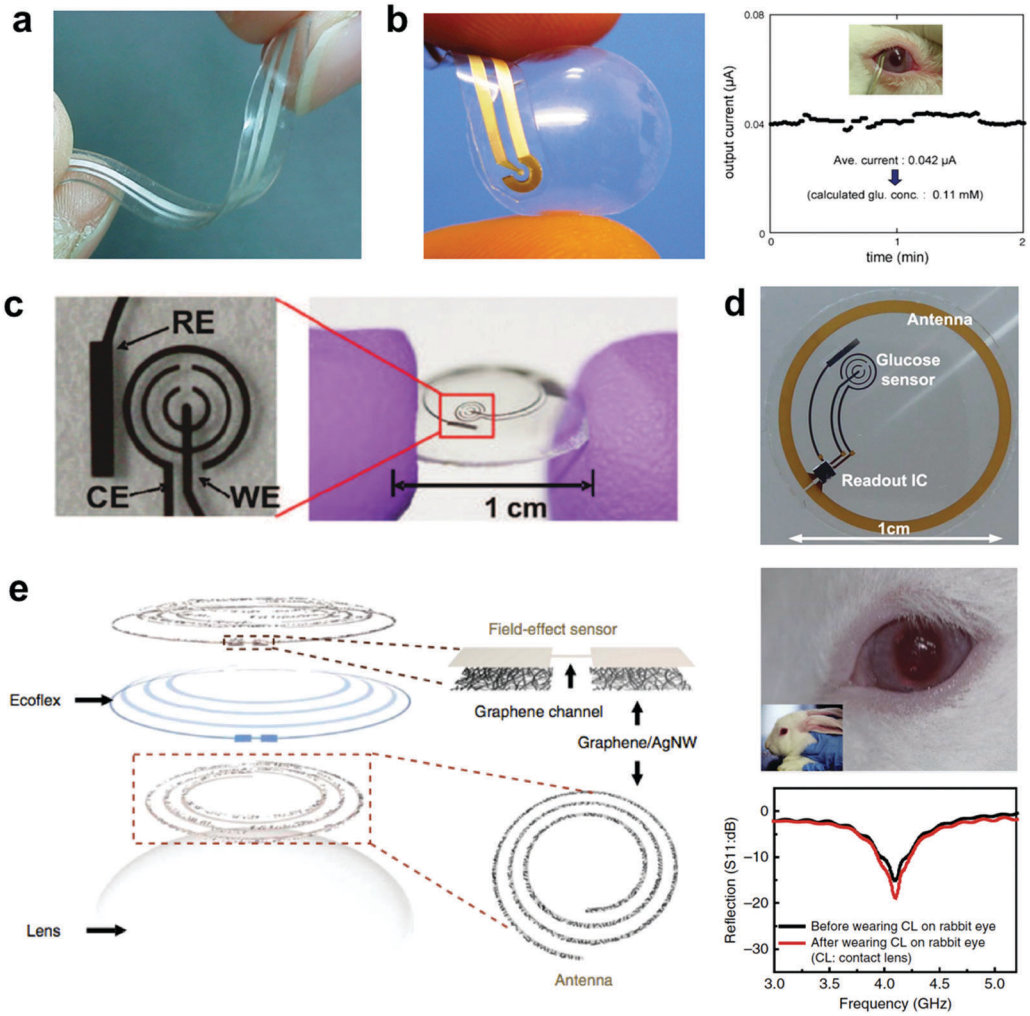

Fig. 6 Wearable and flexible sensors for continuous tear analysis. (a) A flexible PDMS-based tear glucose sensing strip. Reproduced with permission from ref. 111. Copyright 2006 Elsevier. (b) Soft PDMS contact lens with a glucose sensing strip attached. Reproduced with permission from ref. 113. Copyright 2011 Elsevier. (c) Soft contact lens integrated with an amperometric glucose sensor. Reproduced with permission from ref. 114. Copyright 2011 Elsevier. (d) Glucose sensing contact lens, with an integrated antenna for wireless transmission. Reproduced with permission from ref. 115. Copyright 2012 IEEE. (e) Glucose and intraocular pressure sensing contact lens with graphene-hybrid AgNWs to improve the transparency of the lens. Increased reflection after wearing the highly transparent contact lens possibly due to glucose binding in tear fluid. Reproduced with permission from ref. 116. Copyright 2017 Nature Publishing Group.

electrode was bonded to the peripheral surface and GOx was immobilized onto the sensor. The device was tested *in vivo* on a rabbit without using anesthetics. A change in the tear glucose level was observed after oral glucose administration; continuous tear glucose monitoring was performed and the sensor output current remained stable (Fig. 6b). The calculated glucose concentration from the measured current was consistent with human tear glucose concentration. Yao *et al.* furthered this combination of glucose sensor and contact lens by constructing a contact lens with an amperometric glucose sensor.[114] The glucose sensor was created on a polymer substrate and then the substrate was shaped into a contact lens. GOx was immobilized in a titania sol–gel layer that showed improved sensitivity as the titania sol–gel film is very efficient for retaining the GOD activity and preventing the enzyme detachment. A Nafion permselective film was used to reduce potential interference from ascorbic acid, lactate, and urea present in tears. The contact lens was tested in glucose solutions and yielded sensitive measurements with good interference rejection. The same group further improved the functionality of contact lens glucose sensors and enabled continuous and real-time tear monitoring with wireless transmission (Fig. 6c).[114] A loop antenna, a wireless communication interface chip and an electrochemical glucose sensor (Fig. 6d) were integrated on the polymer substrate formed into a contact lens.[115] The gold antenna loop was directly patterned on the polymer substrate and was used for RF powering from a distance of 15 cm. The integrated circuit (IC) was based on a 0.36 mm^2 CMOS chip with no external components. The device was tested in buffer solutions on a PDMS eye model with an artificial tear duct and tear drain, and was able to yield sensitive results continuously in real time. This type of contact lens based glucose sensor has low power consumption (3 μW) and can transmit measurement data with a wireless readout. This platform was later further developed by Google. More recently, Kim *et al.* developed soft contact lenses for wireless detection of glucose and intraocular pressure (Fig. 6e).[116] Using a graphene (2D nanomaterial) hybrid with Ag nanowires (AgNWs) (1D nanomaterial), the conductivity, transparency and stretchability of the contact lens were enhanced, and the hybrid can serve as a source/drain electrode of a field-effect transistor (FET) with graphene as a channel. For glucose sensing, GOx was immobilized on the graphene channel with a pyrene linker; oxidation of glucose and reduction of water to hydrogen peroxide change the concentration of charge carriers in the channels and thus changes the drain current. SU8 was used as an additional diffusive barrier to protect AgNWs from external damage from molecules in tear fluid, as well as to prevent AgCl formation that could be harmful for human eyes. The FET glucose sensor achieved 10 times improvement in sensitivity compared to previous evaporated metal electrodes. The bottom spiral structure is used for glucose sensing while the top spiral structure enables wireless transmission and powering. This wireless sensor was integrated onto the eyes of a live rabbit and showed a higher reflection than the value before wearing due to glucose binding in tear fluid of the rabbit (Fig. 6e). This device fully explored the design with 2D nanomaterials and achieved independent and simultaneous multi-analyte sensing in real time with wireless transmission.

In addition to wearable and flexible electrochemical sensor based tear analysis, the optical sensing strategy was also explored toward tear glucose monitoring. Zhang *et al.* reported a soft hydrogen contact lens with assembled fluorescent nanoparticles with a porous structure.[117] This contact lens was tested in glucose solution. The fluorescence intensity and resonance energy transfer were measured to obtain the glucose concentration. The sensor could be used to monitor glucose levels continuously for at least 5 days. In addition, Badugu *et al.* developed a contact lens embedded with boronic acid-containing fluorophores to perform glucose sensing.[118] Recently, a gelated colloidal crystal array (CCA) attached contact lens was developed.[119] The CCA was embedded in a hydrogel matrix and then attached onto a rigid gas permeable contact lens. The CCA is able to selectively diffract visible light; the change in glucose concentration between 0 and 50 mM will shift the diffracted wavelengths between 567 and 468 nm, corresponding to a visible color change from reddish yellow to green and to blue. The device was tested *in vitro* and yielded observable color changes in glucose solution and good specificity in simulated tear fluid, but the sensitivity was severely affected in simulated tear fluid.

Despite the excellent wearability introduced by the contact lens platform, tear sensing still faces limitations that need to be improved. Transparency of the contact lens is usually reduced by the embedded sensor structure and can obstruct users' vision in daily life. The material selection and nanostructure design, and transparent sensor material combined with careful structure design may be further explored to improve transparency. Heating in the contact lens due to near field wireless powering could also cause discomfort and even irritation in users' eyes, so further research on the selection of antenna material or energy harvesting methods (*e.g.* biofuel cell) could be useful to resolve this issue. Another limitation is the readout distance of the near field wireless communication. The wireless readout distance in the works of Liao *et al.* and Kim *et al.* was 15 cm and 10 mm, respectively. This means that the users need to hold the readout device very close to eyes, which might not be practical for prolonged continuous monitoring. Some other issues to consider include the need for glucose monitoring during sleep (when hypoglycemia, a dangerous situation for diabetics, could occur), potential temporal variations in tear glucose concentration and calibration for such variations, and possible pupil damage related to contact lens wear such as microbial keratitis, contact lens peripheral ulcers and inflammatory complications.[120]

3.3. Saliva analysis

Human saliva has been considered as an attractive biofluid for non-invasive diagnostics and monitoring.[121,122] It is a clear and viscid biofluid secreted into the mouth by salivary glands and the fluid contains various biomarkers, such as glucose, lactate, phosphate, enzymes (*e.g.* alpha-amylase (sAA)), hormones (*e.g.* cortisol, steroids), antibodies (*e.g.* IgA, IgG), *etc.*[123] Salivary cortisol and sAA have been identified as crucial biomarkers for

physical and psychological stress; antibodies in the saliva are shown to be useful tools for disease diagnosis (*e.g.* HIV and intestinal infections); some protein and mRNA biomarkers (*e.g.* IL-8 and KRAS) in saliva were identified as cancer biomarkers and can distinguish cancer patients from healthy individuals.[123–133] Investigation of these salivary biomarkers was facilitated by the abundant availability of saliva and the ease of saliva sample collection. Earlier investigation was conducted through sensing analyte concentrations in *ex vivo* human saliva samples collected by spitting or with a collection paper strip.[134,135] Sample collection is then followed by sensing out of the body, either in lab tests or in a portable device.[123–133,136,137]

As the interest in saliva sensing grew over the past years, wearable devices for *in situ* saliva analysis were developed (Fig. 7). The sample collection and sensing processes were integrated into a single wearable and flexible platform. Mannoor *et al.* developed a salivary bacteria sensing platform on tooth enamel (Fig. 7a).[138] Self-assembled antimicrobial peptides on graphene selectively bind to bacteria in saliva, and the binding process alters the electrical resistance that allows for bacterial quantification (Fig. 7a). The graphene nanosensors were printed onto water-soluble silk thin-film substrates and then integrated with electrodes patterned with an inductive coil antenna. The graphene/electrode/silk hybrid structure is capable of detecting highly sensitive single-bacteria and a wireless readout could be achieved with the active device in proximity. In addition to the form of sensor attachment, the mouthguard was taken as another form factor for collection–sensing integration. Kim *et al.* demonstrated an integration of printable enzymatic electrodes on a mouthguard.[139] Lactate oxidase was immobilized on the working electrode, and the 3-electrode system was screen printed onto the mouthguard. The lactate concentration was measured amperometrically, and the *ex vivo* experiments showed promising results for continuous on-body saliva monitoring. The same group further explored this electrochemical mouthguard platform toward salivary uric acid (UA) measurements (Fig. 7b).[140] The printed working electrode Prussian blue transducer was chemically modified by crosslinking uricase enzyme with electropolymerizing *o*-phenylenediamine (Fig. 7b). The sensor was fabricated on a flexible PET substrate and then integrated with a wireless amperometic circuitry and mounted onto the mouthguard. This mouthguard UA sensor was tested on saliva samples from hyperuricemia patients and healthy subjects. The detected salivary UA levels were much higher in hyperuricemia patients than in healthy subjects. Although real-time in-mouth monitoring was not discussed, the sensor yields sensitive amperometric measurements of UA and real-time bluetooth wireless data transmission was achieved. Arkawa *et al.* also integrated biosensing and real-time wireless communication on a monolithic mouthguard (Fig. 7c).[141] Glucose oxidase was entrapped with poly(MPC-*co*-EHMA) (PMEH) onto the working electrode, and the 3-electrode system was combined with a wireless transmitter onto a polyethyleneterephthalateglycol (PETG) mouthguard. The electrode area and PMEH coating on the glucose sensor were optimized to increase the output current response to glucose binding. The sensor was tested with a phantom jaw in an open-loop artificial saliva injection system and the results were wirelessly transmitted to a personal computer (Fig. 7c). The testing yields sensitive amperometric outputs over relevant glucose levels in human saliva.

As described above, wearable saliva sensors have been developed towards continuous in-mouth monitoring. While saliva is an attractive candidate for non-invasive health monitoring, there are still several major roadblocks for practical implementation of saliva sensing. Considering the continuous in-mouth use of wearable saliva sensors, the materials, devices and systems

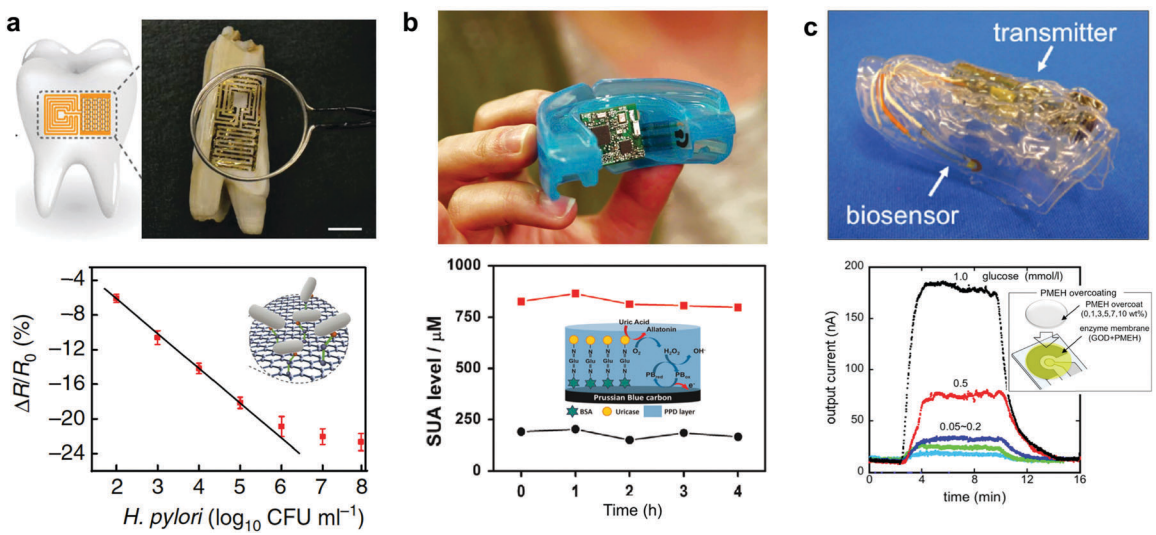

Fig. 7 Wearable and flexible sensors for saliva analysis. (a) Bacteria sensing on tooth enamel with graphene-based nanosensors. Bacteria quantification was performed based on electrical resistance variation. Reproduced with permission from ref. 138. Copyright 2012 Nature Publishing Group. (b) Mouthguard device with electrochemical sensors to measure salivary uric acid (sUA) concentration. Enhanced sUA level was detected in hyperuricemia patients. Reproduced with permission from ref. 140. Copyright 2015 Elsevier. (c) Saliva glucose sensing with the mouthguard sensing platform where GOx was entrapped in PMEH. Reproduced with permission from ref. 141. Copyright 2016 Elsevier.

should be fully biocompatible. In the continuous monitoring scheme, the abundance of secreted proteins and active chemicals generated from food residues can result in significant interference with target analyte sensing, so the saliva sensor should be of high specificity in this complex and dynamic chemical environment. Another challenge comes from contamination and sensor damage. Bacteria accumulate quickly on surfaces inside the oral cavity due to the favorable humidity and temperature conditions in the mouth. If the sensor is unprotected, a bio-film will form on the sensor surface and severely affect the sensitivity of the device. An antimicrobial or protective coating on the sensor surface might resolve this issue, but enhanced sensor sensitivity might be necessary after the introduction of such protective coatings. Voluntary and involuntary mouth muscle movements in daily life (*e.g.* talking) may also impose mechanical stress on sensors, so the sensors should be mounted in the mouth securely while remaining durable in lieu of mechanical stress. Considering all these challenges, the future effort on wearable saliva sensors should focus on careful design of the form factors that house sensors, ensuring materials' biocompatibility, sensor function and accommodating user's comfort and convenience at the same time.

3.4. Non-invasive blood analysis

Blood is a body fluid that transfers necessary substances such as nutrients and oxygen to cells and transports metabolic waste products out of cells. It sustains the physical and chemical equilibrium of cells. A blood test has been the gold standard for many clinical diagnostic applications.[142–144] In particular, blood glucose has been heavily investigated and monitored for diabetic regulation. Various devices were developed to sense and monitor biomarkers in the blood.[145–149] Since blood is contained in blood vessels with less accessibility, earlier devices either performed analysis based on invasive blood draw or required implantable sensors that are undesired for continuous health monitoring.

Wearable devices for non-invasive blood monitoring were recently developed, mostly for oxygenation sensing, pressure sensing, and heart rate detection. The widely available commercial product for noninvasive molecular blood sensing is the pulse oximeter, which performs pulse oximetry on finger tips, an optical test that measures changes in the optical properties of hemoglobin in its oxygenated and deoxygenated states and yields both the oxygen saturation level and blood pulse. The pulse oximetry level has close clinical relevance in the management of acute and chronic respiratory disease.[150–152] The earlier versions of pulse oximeters were of portable size, and more pulse oximeters were developed to reduce the oximeters into wearable size. Haahr *et al.* developed an electronic patch that can perform reflectance pulse oximetry.[153] The electronic patch integrated a photodiode (sensor), a battery, and a PCB in an adhesive patch; the chip on PCB allows for wireless communication. The microsystem could be attached to different parts of the skin surface. Since many conventional pulse oximetry systems are transmission-based detection systems, sensors were applied to thinner or peripheral parts of the body which are less opaque, but in the case of shock-induced centralization and a resulting drop in perfusion, peripheral detection would not yield reliable results. To resolve this limitation, Venema *et al.* developed a reflection-mode oxygen saturation sensor that could be worn in the ear canal like a headphone.[154] The sensing was based on photoplethysmography (PPG), which allowed for reflectance pulse oximetry at opaque body parts. Human subject testing showed that the device was very comfortable for long-time wearing, and the tight-fit ear mold could reduce the motion artifact, and in-ear detection capability provided stable and more reliable results than peripheral detection. The pulse oximetry devices described above were rigid and made of inorganic sensors. Recent advances in flexible and conformal electronics provide attractive routes for accurately assessing the blood oximeter. Lochner *et al.* developed a pulse oximeter sensor with organic materials on flexible substrates (Fig. 8a).[155] The green and red light-emitting diodes (LEDs) and photodiodes were both made of organic materials, and the device was low-cost and disposable. The all-organic optoelectronic sensor accurately measured pulse oxygenation with an error of 2%. Yokota *et al.* reported ultraflexible organic photonic skin with multicolor highly efficient polymer light-emitting diodes (PLEDs) and organic photodetectors (OPDs) for reflective pulse oximeter monitoring (Fig. 8b).[156] The optoelectronic skins are extremely thin (only 3 μm in thickness), lightweight and stretchable; they can endure bending radii of 100 mm or less and repeatedly sustain up to 60% compression. The sensor successfully measured the blood O_2 concentration when laminated on the finger. Recently, Kim *et al.* developed a miniaturized flexible and wearable pulse oximeter (Fig. 8c).[157] Built on a silicone elastomer, the sensor was around the size of a finger nail and was very flexible. It was equipped with a near-field wireless chip that allows for wireless power harvesting and data communication. The device can operate continuously for up to 3 months and can measure oxygen saturation at almost any part of the body, including the earlobe. The stable and robust bonding between the device and the near-field wireless chip allows for wireless power harvesting and data communication. The stable and robust bonding between the device and encapsulation layer can serve as an excellent shield against ambient light. It should be noted that considering that most of the skin/fingernails can introduce motion artifacts and the opaque reflectance mode measurements are susceptible to motion artifacts, signal-processing algorithms should be used to minimize the motion-induced errors.[158,159]

In addition to blood oxygen sensing, non-invasive monitoring of other blood biomarkers (such as glucose and lactate) using wearable devices was also investigated, mainly through optical methods such as Raman and near-infrared spectroscopy. The details could be found in this review.[160] For example, Yadav *et al.* reported a sensor patch using a near-infrared (NIR) LED and a photodiode to measure the diffuse reflectance spectra of blood.[161] The *in vivo* results of this sensor patch showed a significant difference in the blood glucose level before and after a meal, indicating the potential of using NIR for glucose monitoring. Recently a chemical-free blood lactate sensor was developed with the use of microwave-range electromagnetic

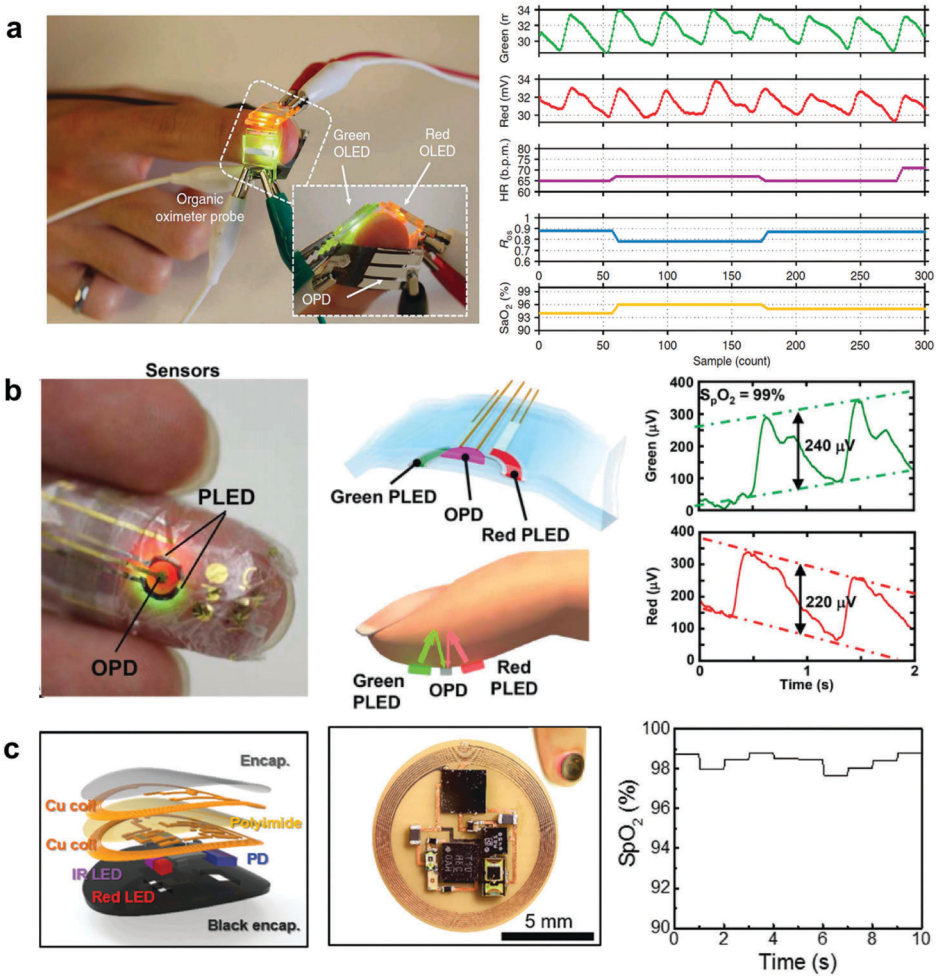

Fig. 8 Wearable and flexible pulse oximeters. (a) Flexible all-organic optoelectronic pulse oximeter with a polymer LED and organic photodetectors. Reproduced with permission from ref. 155. Copyright 2014 Nature Publishing Group. (b) Ultraflexible organic photonic skin with a multi-color polymer LED. Reproduced with permission from ref. 156. Copyright 2016 American Association for the Advancement of Science. (c) Miniaturized flexible pulse oximeter built on silicone elastomer and equipped with a near-field wireless chip. Reproduced with permission from ref. 157. Copyright 2017 Wiley.

(EM) waves.[162] However, these devices usually suffer from poor signal-to-noise ratios and are limited by calibration issues and physiological factors. A significant improvement is needed to replace the conventional blood glucose monitors.

3.5. Interstitial fluid (ISF) analysis

Despite the exciting progress in blood sensing, most chemical analytes in the blood are still inaccessible non-invasively. To bypass this sampling issue, researchers have looked at monitoring the interstitial fluid (ISF) as a way to gain information on chemical concentration in the blood. The composition of the ISF is very similar to blood in terms of small molecules such as salts, proteins, glucose, and ethanol.[163] Over the years, the ISF has been used for non-invasive diagnosis of metabolic disorders, therapy assessment, and organ failure assessment.[164–167] Numerous attempts were invasive with the use of implantable devices. Yuen *et al.* also developed an implantable glucose sensor with surface enhanced Raman spectroscopy (SERS).[168] Silver films over nanosphere surfaces functionalized with a mixed self-assembled monolayer (SAM) were implanted in a rat and the glucose concentration was monitored.

Non-invasive ISF monitoring devices based on reverse iontophoresis (Fig. 9a) were investigated. Reverse iontophoresis, similar to iontophoresis, applies a potential difference between two electrodes on the skin. Ions in the body such as Na^+ act as charge carriers and substances within the body can be extracted through the skin. Since the skin has a net negative charge at physiological pH, an electro-osmotic flow occurs along with the iontophoretic current. Neutral molecules such as glucose can be extracted to the cathode with Na^+ out of the skin.[169,170] The most well-known FDA-approved glucose sensing device, GlucoWatch, utilized reverse iontophoresis to bring the ISF through the skin to the externally attached sensor. The GlucoWatch was a highly integrated wrist-watch device that features both reverse-iontophoresis and biosensing. Amperometric electrochemical sensors were screen-printed; hydrogel discs with GOx at a concentration gradient served as the reservoir for the collected glucose. In spite of the excellent integration of its features, the GlucoWatch requires a certain minimum duration for sufficient

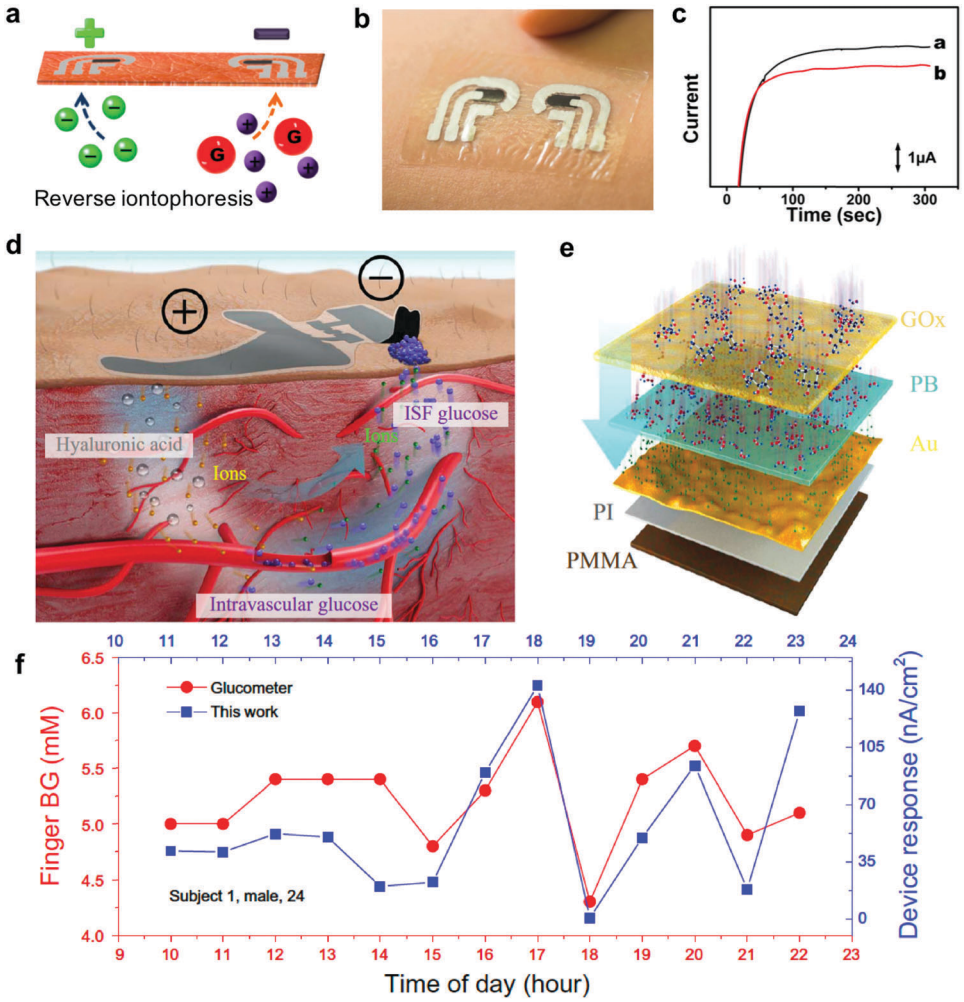

Fig. 9 Wearable sensors for non-invasive monitoring of the interstitial fluid (ISF). (a) ISF sensing mechanism with the use of reverse iontophoresis. Reproduced with permission from ref. 173. Copyright 2015 American Chemical Society. (b) All-printed tattoo-based ISF glucose sensor. Reproduced with permission from ref. 173. Copyright 2015 American Chemical Society. (c) Tattoo-based sensor measured pre- and post-meal ISF glucose level on a human subject. Reproduced with permission from ref. 173. Copyright 2015 American Chemical Society. (d) Application of electrochemical twin channels (ETC) for increasing intravascular glucose transport into ISF and for increasing the flux of reverse iontophoresis. Reproduced with permission from ref. 174. Copyright 2017 American Association for the Advancement of Science. (e) Biosensor layout for the ETC-based ISF glucose monitoring system. Reproduced with permission from ref. 174. Copyright 2017 American Association for the Advancement of Science. (f) Human subject testing of the ETC-based ISF glucose monitoring system over a day, with concurrent finger-pricked blood glucose measurements. Reproduced with permission from ref. 174. Copyright 2017 American Association for the Advancement of Science.

glucose extraction and it still suffered from inaccuracy,[171,172] interference from sweating,[160] and the product was removed from the market due to filed reports on skin irritation and blisters during continuous usage.[160] The reverse iontophoresis technique was also used in other ISF sensors. Bandodkar *et al.* introduced an all-printed flexible temporary tattoo-based glucose sensor (Fig. 9b).[173] Both sensing electrodes and reverse-iontophoresis electrodes (and agarose hydrogel coating) were printed onto a tattoo paper, and the use of a GOx-modified Prussian blue transducer allowed for the detection at a lower potential than the GlucoWatch. The current density required for ISF extraction was also significantly lower than the GlucoWatch. The device was tested on healthy individuals for pre- and post-meal glucose monitoring, and the results showed the rise in the glucose level after a meal (Fig. 9c). Recently, Chen *et al.* developed a flexible and non-invasive ISF glucose monitoring system with electrochemical twin channels (ETC) and reverse iontophoresis.[174] With the use of ETC, high-density hyaluronic acid (HA) is transdermally repelled into the ISF under the anode; the extra HA (positively charged) raises the ISF osmotic pressure and thus promotes intravascular blood glucose transport into the ISF (Fig. 9d). The increased glucose concentration in the ISF can then increase the flux of reverse iontophoresis at a low-current level. As a result, more "real" blood glucose is measured and the blood–ISF glucose correlation is improved. The biosensor consists of layers of poly(methyl methacrylate) (PMMA), polyimide (PI), a sand-dune nanostructured gold thin film, a transducer layer (PB), and a transfer/glucose oxidase (GOx) immobilization layer (Fig. 9e). The device was tested on human subjects with hourly measurement during a 1 day period,

and the results showed a good match and a high correlation between the ISF and blood glucose level, with a 1 hour time lag in the ISF glucose concentration (Fig. 9f).

In addition to reverse iontophoresis, ISF extraction could be achieved with sonophoresis, which employs 20 kHz ultrasound to increase the permittivity of the skin to the interstitial fluid. The glucose in the ISF then flows to the skin for electrochemical sensor detection.[175] But this technique creates micropores in the skin and was considered minimally invasive. Based on this technique, Pu *et al.* developed a polyimide-based flexible electrochemical sensor integrated with an ISF-collecting microfluidic chip for continuous glucose monitoring.[176] The authors thus worked to increase the sensitivity at lower glucose concentration by modifying graphene onto the working electrode with inkjet printing and introducing gold nanoparticles onto the graphene layer to improve uniform and enhanced electrochemical activity and electron transfer rate.[177] *In vitro* testing showed promising results for continuous glucose monitoring but on-body testing was not yet accomplished. In addition to glucose monitoring, ethanol was also continuously monitored using a wireless wearable device *via* poration of the stratum corneum of the skin.[178] Micropores (open for 3 days) with the diameter of human hair were created by a handheld porator, and an ISF harvesting system was positioned on the pore location to collect the fluid with an electromechanical pump in the harvesting unit. The electrochemical sensor inside the harvesting unit then measured the ethanol concentration. Using a similar extraction method, Venugopal *et al.* reported a wearable sensor for the continuous assessment of cortisol using electrochemical impedance spectroscopy in the ISF.[179]

As described above, there is great potential for ISF-based biomarker monitoring, but several limitations should be noted and addressed. The delay of glucose and ethanol response either due to diffusion from the blood to the ISF or due to ISF extraction and collection may impose delayed detection of dangerous conditions (*i.e.* hyperglycemia or hypoglycemia). Skin irritation due to continuous ISF extraction is also an issue to be addressed. Sporadic sampling with on-off switch or the use of smaller reverse iontophoresis current with conformal design for ISF extraction may be applied to reduce such adverse effects. In addition, interference from external glucose sources (*i.e.* sweat glucose and glucose residue on skin) could impose inaccurate readings; inconsistent ISF extraction efficiency over the collection area or over time may also introduce inconsistency in the measured results. Finally, a fully integrated sensing platform is yet to be constructed, which requires sensor powering, signal processing, and wireless communication.

3.6. Wound monitoring

Would healing undergoes three stages, including vascularization, granulation, and re-epithelialization stages. In the vascularization stage, growth factors and other proteins are released and form a temporary matrix on the wound; in the granulation stage, various biological components are secreted; in the re-epithelialization stage, cell apoptosis and destruction of the provisory matrix tissue occur.[180] The chemical composition of wound exudates changes significantly over the three stages and is crucial for proper healing, and relevant parameters such as pH, uric acid and C-reactive protein (CRP) concentration of wound exudates could indicate the stage of healing and the presence of infection.[181–186] Monitoring the wound healing process (wound management) can reduce hospitalization time, prevent amputations, and aid in therapy studies. Of all wound-related morbidities, chronic ulcer has affected 25% of diabetics and is the leading cause of non-traumatic amputation in developing countries;[187] it also occurs in around 1–2% of the American population.[188] Chronic ulcers can be especially difficult to treat and highly susceptible to infection. The use of wound management would benefit these patients tremendously. Qualitative wound assessment was done by visual inspection, which could be subjective and sometimes yields inconsistency due to variation in lighting and angle. Quantitative assessment of wound parameters was investigated over the years and wearable wound management devices were constructed to monitor parameters such as pH, CRP concentration, hydration, skin temperature, *etc.*[189] Earlier wearable device based wound monitoring was integrated as a system with a wound dressing patch.[190] Voirin and coworkers utilized the optical detection method to measure pH and CRP concentration. PHEMA/DMAEM hydrogels change volume in response to pH variation, and OptoDex coating on the substrate was used as a receptor for CRP. A sensitive layer was deposited on a waveguide substrate; changes in hydrogel volume and specific adsorption of CRP by the OptoDex coating lead to a varied refractive index of the interface. This change in refractive index was then detected using a spectrometer. The device was used to monitor changes in pH and CRP concentration in serum and observable changes were recorded.

Over the recent years, flexible sensors for continuous wound monitoring were demonstrated. Mehmood *et al.* developed a flexible telemetric sensing system to monitor pressure, temperature and moisture of wound.[191] Interfaced with off-the-shelf sensors, a flexible circuit was fabricated and wireless RF data transmission was achieved. Hattori *et al.* developed a sensor platform that can softly and reversibly laminate at wounds and micro-metal resistors provide precise measurement of temperature and thermal conductivity of the skin near the wounds.[192] The measurements were processed on a computer with 3D FEM to yield time-dependent mapping of temperature and thermal conductivity data. Punjiya *et al.* constructed a smart bandage platform in chronic wound healing (Fig. 10a).[193,194] The smart bandage measures wound pH with pH sensitive polyaniline (PANI) coated threads, which increases the open circuit potential when pH is lowered. Custom CMOS readout electronics were used for wireless readout, and 2D pH mapping was achieved. Guinovart *et al.* introduced a resistive pH wound monitoring device that uses modified screen-printed Ag/AgCl electrodes on a commercial bandage (Fig. 10b).[195] A PVB coated membrane was used on the reference electrode (which displayed a more stable potential compared to the bare solid Ag/AgCl reference electrode), and the working electrode consisted of PANI, which has potentiometric change due to pH change based on the transition between emeraldine salt and emeraldine base.

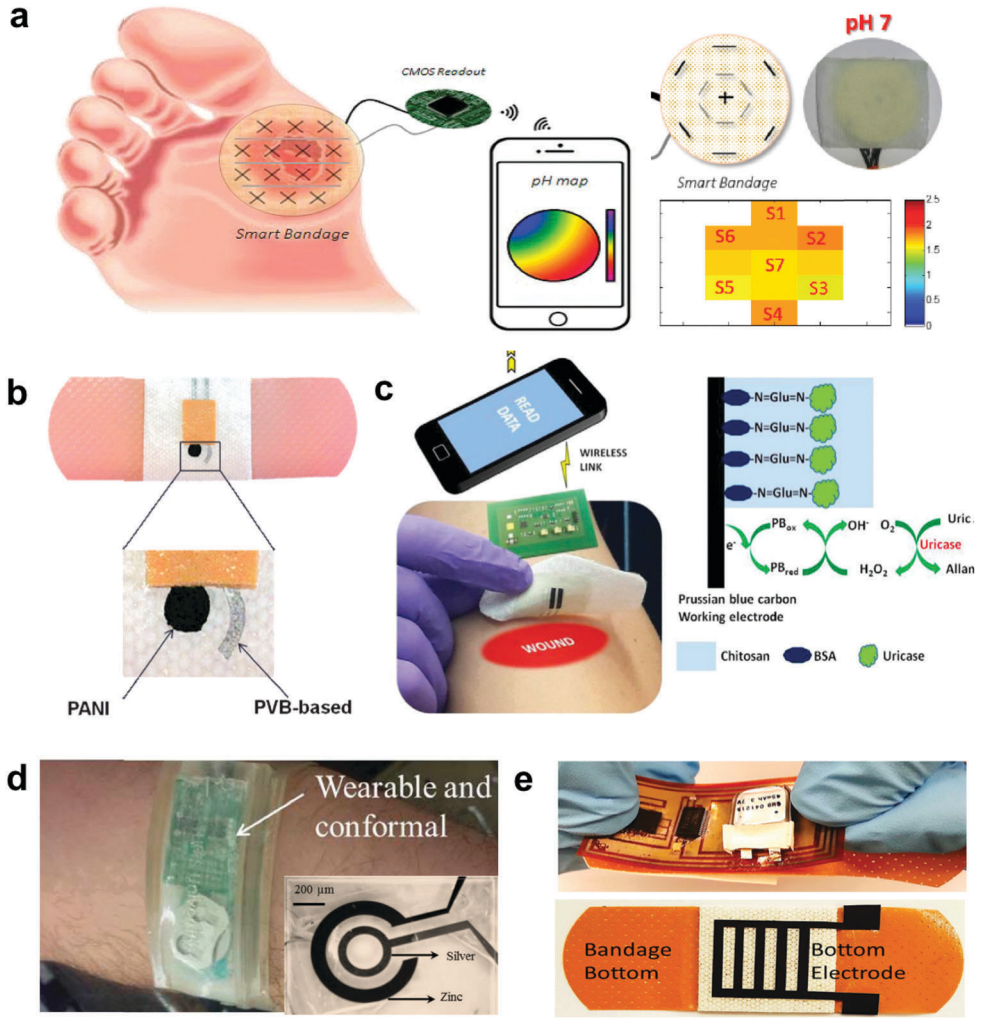

Fig. 10 Wearable sensors for wound monitoring. (a) Smart bandage for chemical sensing of wound pH using pH-sensitive PANI coated threads. CMOS wireless readout and 2D mapping of pH levels were incorporated. Reproduced with permission from ref. 193 and 194. Copyright 2017 IEEE. (b) Wound pH wound monitoring with the PANI working electrode and the PVB-coated reference electrode. Reproduced with permission from ref. 195. Copyright 2014 Wiley. (c) Wound uric acid sensing bandage with wireless readout. Uricase was immobilized on carbon working electrodes modified with Prussian blue. Reproduced with permission from ref. 196. Copyright 2015 Elsevier. (d) Wound oxygen monitoring with a smart bandage encased in a 3D-printed flexible platform. Zn–Ag electrodes were used for oxygen sensing. Reproduced with permission from ref. 199. Copyright 2015 IEEE. (e) Inkjet-printed smart bandage for continuous monitoring of irregular bleeding, pH and external pressure using capacitive and resistive sensing. Reproduced with permission from ref. 200. Copyright 2016 Nature Publishing Group.

Kassal *et al.* constructed a uric acid sensing bandage with a wireless connection feature.[196] Prussian blue (PB) modified carbon electrodes were screen printed onto a commercial bandage, and uricase was then immobilized on the working electrode (Fig. 10c). Uric acid (UA) oxidation produces hydrogen peroxide, which was reduced catalytically by the PB-carbon electrode; in this way, UA detection was achieved at a very low negative working potential. The bandage was connected to a potentiostat that measures and stores biosensor current output and transfers data wirelessly. Liu *et al.* fabricated a uric acid sensor with conductive thread and coated the polyester thread with Ag/AgCl or carbon ink.[197,198] Sensors were then embroidered and uricase was immobilized onto the working electrode. The embroidered structure has stable and consistent output in simulated wound fluid between flat and bending conditions. Mostafalu *et al.* demonstrated a smart bandage encased in a stretchable and flexible 3D-printed platform for wound oxygen monitoring (Fig. 10d).[199] Silver and electroplated zinc electrodes on parylene-C were used for oxygen sensing, and a thin layer of PDMS was used as an oxygen-selective membrane for the sensor. Farooqui *et al.* utilized an inkjet-printed smart bandage to continuously monitor irregular bleeding, pH and external pressure and wirelessly transmit output data (Fig. 10e).[200] Capacitive sensing was used for bleeding and pressure sensing: irregular bleeding causes a change in the dielectric constant between two electrodes on either side of the bandage strip; pressure leads to a change in the distance between the two electrodes. Resistive sensing was used in pH measurements: the conductivity of the carbon-based electrode varies when the electrode is exposed to solutions of different pH, and the change in resistance is

measured for pH sensing. A double-sided detachable PCB was inkjet printed on Kapton adhesive tape, and an on-chip microcontroller was used to store measured data. The device was tested on human skin and it exhibited great mechanical resilience and displayed a text of ''change bandage'' when bleeding happened on the site. Melai *et al.* used the graphene oxide coated working electrode on a screen-printed substrate to monitor pH in wounds.[201] A simultaneous pH and glucose sensing wound patch was recently developed.[202] The parameters were measured *via* measuring fluorescence signals from a pH indicator sensitive dye-carboxynaphtho-fluorescein probe, and a metabolite-sensing enzymatic system (based on glucose oxidase and horseradish peroxidase) that responds to glucose concentration. The system was able to detect low glucose concentration in artificial wound exudate. Since the results could be seen by visual inspection of the fluorescence intensity, it provides direct and qualitative wound status information to users, and can help to distinguish between an autonomously healing and a chronic wound at an early stage.

Although multiple wearable devices have been developed to provide useful information on wound healing, multi-parameter sensing was yet to be achieved to give a more comprehensive understanding of the wound healing status. The devices described above either performed *in vitro* testing on wound exudate or on human skin for a relatively short time, and thus did not examine if wearing such modified bandages for long time may have adverse effects on the wound healing process or lead to discomfort for users. Since the wound healing process spans over at least a few days, continuous monitoring could be achieved by sporadic sampling, but the replacement of sensor-bandages would require high consistency in sensing performance between individual sensor-bandage. If the same piece of bandage could stay on wound for extended time, storage of measured data or real-time wireless data transmission to an external device is needed for the temporal progress of the wound healing status.

3.7. Breath analysis

Breath is the gas–vapor mixture that humans exhale through either nasal or oral cavity. The potential for breath measurement is enormous, since it is completely noninvasive and inherently safe.[203] Breath collection can be done on any individual who can breathe, even including neonates and Alzheimer patients. The composition of breath is complex: it includes a mixture of nitrogen, oxygen, CO_2, and water vapor. The remainder includes as many as 500 different compounds, either endogenous (produced by physiological processes) or exogenous (ingested food, air, *etc.*). Among these endogenous compounds are acetone, carbon monoxide, ammonia, and nitric oxide.[204] The breath carbon monoxide test has been used for neonatal jaundice diagnosis; breath ammonia can be used for assessment of asthma and hemodialysis; the breath nitric oxide test was used to monitor the asthma therapy process; breath acetone could be used for diabetes monitoring in place of finger-pricking, *etc.*[204–208] In addition to breath vapor composition, breath rate and breath condensate are also used for analysis. The breath rate profile is a useful analysis for individuals with sleep apnea, asthma, and chronic obstructive pulmonary disease (COPD).[204,209,210] Breath condensate, a liquid mixture of chilled breath, contains fluids from airway-lining and pulmonary tissues. Species such as cytokines, reactive oxygen chemicals, and leukotrienes were found in breath condensate and could be used for disease diagnosis and monitoring.[204,209,210]

Breath sensing technology has been developed since the 1970s, and most sensing processes require bulky equipment for breath collection. A portable breath sensing device was developed in the late 2000s: using the electrostatic self-assembly of super-hydrophilic SiO_2 nanoparticles, Corres *et al.* built a humidity sensor and integrated it into an optical fiber.[211] The sensor performance has good reproducibility and low hysteresis; when the sensor was coupled with methylene blue dye, fast response was achieved and characteristic hyperventilation respiration patterns were detected. A portable breath acetone sensor was developed.[212] The Si-doped epsilon-WO_3 nanoparticle was used as the sensing material due to its high sensitivity and selectivity to acetone at high relative humidity, which enabled low-concentration detection of acetone. Si-Doped epsilon-WO_3 nanostructured films were flame-deposited and annealed *in situ*. During human testing, the sensor measured acetone concentration continuously when the test person was at rest and during physical activity. The results were sensitive and consistent with those detected by the standard proton transfer reaction mass spectrometry (PTR-MS) technique. Borini *et al.* also developed a flexible breath humidity sensor with graphene oxide (Fig. 11a) at a wearable size, and measured the sensor performance using a controlled humidity generator.[213]

The impedance of the graphene oxide sensor varies according to the relative humidity and temperature. The 2D graphene oxide film at 15 nm thickness reached ultrafast response to a modulated humid flow ($\sim$30 ms response and recovery time) and maintained full-scale output at the same time. The device is highly flexible (Fig. 11a) and transparent, and its wearable size and low cost of production made it a good candidate for continuous breath analysis. The sensor response can also distinguish different patterns of human behaviors (speaking *vs.* breathing, whistle tunes by different users), which may be useful for user recognition in breath monitoring. Using the humidity change as an indicator of exhalation, Caccami *et al.* measured the graphene oxide resistance change to monitor respiratory activity in real time (Fig. 11b).[214] A flexible antenna was prototyped on Kapton to enable RFID and wireless data transmission. The antenna and the graphene oxide sensor were integrated onto a facemask, and this wearable device was tested on a subject. The results showed its ability to monitor individual exhalation–inhalation peaks and distinguish normal breath from apnea conditions. Wang *et al.* developed a flexible chemical sensor for breath acetone measurement (Fig. 11c).[215] Using a 3D biomimetic design resembling a hierarchical butterfly wing, a porous chitosan–graphene oxide biocomposite was synthesized. The structure allows for excellent mechanical strength and flexibility in addition to biocompatibility and electronic activity. This biocomposite layer was sandwiched

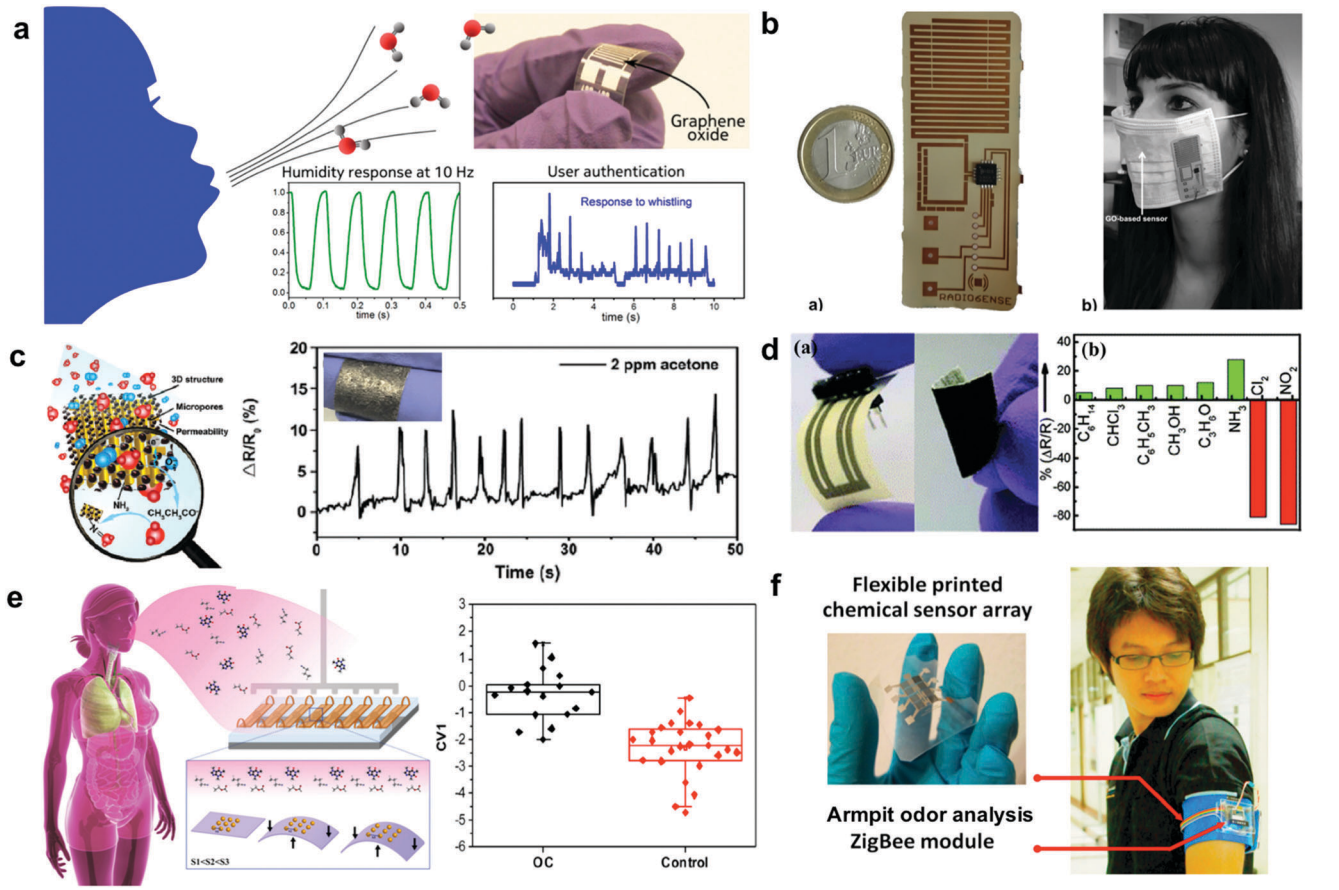

Fig. 11 Wearable and flexible sensors for gas/breath analysis. (a) Graphene-oxide-based flexible breath humidity sensor capable of measuring breath humidity and distinguishing human behaviors such as whistling. Reproduced with permission from ref. 213. Copyright 2013 American Chemical Society. (b) Graphene-oxide-based sensor for respiratory activity (breath humidity) monitoring. A flexible antenna was integrated for RF identification and wireless data transmission. The device took the form of a face mask. Reproduced with permission from ref. 214. Copyright 2017 IEEE. (c) Flexible acetone chemical sensor based on a porous chitosan–graphene oxide biocomposite. Impedance variation was observed under pulsated ejection of simulated diabetic breath. Reproduced with permission from ref. 215. Copyright 2017 Royal Society of Chemistry. (d) Flexible inkjet-printed single-walled carbon nanotube (CNT) based chemical sensor for Cl_2 and NO_2 sensing. Decrease in sensor resistance was observed for Cl_2 and NO_2 vapor, compared to other common gas vapors. Reproduced with permission from ref. 216. Copyright 2012 American Chemical Society. (e) Flexible exhaled breath sensor-array based on modified gold-nanoparticles for ovarian carcinoma (OC) diagnosis. Discriminant factor analysis (DFA) separated breath samples collected from subjects with OC as well as from controls. Reproduced with permission from ref. 221. Copyright 2015 American Chemical Society. (f) Flexible printed CNTs/polymer sensor-array for armpit odor monitoring (*e.g.* ammonia, acetic acid).[223] Reproduced with permission from ref. 223. Copyright 2014 MDPI.

between copper electrodes and paper substrate and the impedance changed according to acetone concentration. The sensor was implemented as a flexible wristband and tested with pulsated ejection of simulated diabetic breath flow over the sensor (2 ppm acetone vapor with 85% relative humidity). The sensing results were calibrated with relative humidity to prevent overestimation of acetone concentration. The device exemplifies great sensitivity and specificity in real-time acetone monitoring. Ammu *et al.* used inkjet-printed single-walled carbon nanotube (CNT) films on PET and cellulosics (Fig. 11d) substrates to detect nitrogen dioxide and chlorine.[216] The penetration of the gas molecules into the CNT films increases the distance between the conducting pathways of CNTs, causing the resistance changes of the sensor. The inkjet-printed CNT films showed a decrease in resistance for NO_2 and Cl_2 as compared to an increase in resistance for other common gas vapors (Fig. 11d). Without the use of the vapor concentration process, NO_2 vapor was detected at as low as 125 ppb and Cl_2 vapor was detected at as low as 500 ppb in ambient air. The inkjet printing process helped to control the film thickness and maintain consistency among sensors. The group experimented with CNT films printed on a PET substrate and CNT films printed on cellulosics (paper and cloth) to test sensor recovery performance: the cellulosic substrates aided in spontaneous gas recovery in an ambient environment at room temperature, and the PET substrates required photoirradiation for sensor recovery.

In addition to single-analyte sensing, the aggregation of chemical sensors into arrays was complemented with multivariate data analysis to yield quantification and identification of compounds with combinatorial selectivity. Recognition of a specific compound or a specific mix of compounds is done by all sensors, which is parallel to the behavior of the human olfaction sensor. Due to this similarity, these gas sensor arrays were called "electronic noses" ("e-nose"). The concept was

demonstrated in the early 1980s but used for gas analysis. Since the early 2000s, electronic noses have been used in breath analysis, especially for classification of individuals into pathology of interest. Many studies have used electronic noses for diagnosis of diseases such as lung cancer, pneumonia, asthma, COPD, tuberculosis, kidney functions, neurological diseases, *etc.*[217–219] Based on this electronic nose concept, Seesaard *et al.* developed a fabric-based wearable chemical amine sensor prototype with carboxylic-functionalized single-walled carbon nanotube/polymer (SWNT–COOH) nanocomposite.[220] 4 types of polymers were used to sense different analytes such as ethanol, ammonium hydroxide, pyridine, *etc.* The composite solution was drop-coated onto interdigitated electrodes prepared by embroidery of conductive thread into fabrics. The fabricated sensor array was used for odor analysis of two individuals on their urine, armpit and exhaled breath samples *ex vivo*. Principal component analysis (PCA) discrimination showed that the fabricated electronic nose was capable of distinguishing the odor profile of two different individuals. Haick and coworkers introduced a flexible sensor array based on molecularly modified gold nanoparticles for diagnosis of ovarian carcinoma (OC) from exhaled breath (Fig. 11e).[221] The flexible sensor could selectively detect ppb level of volatile organic compounds (VOCs) that are related with ovarian cancers in exhaled breath and could distinguish them from environmental VOCs. Through the use of discriminant factor analysis (DFA) based on the leave-one-out method, in actual breath samples from subjects with OC as well as from controls, the sensitivity, selectivity and accuracy were found to be 81.3%, 82.9% and 83.6%, respectively. The same group further developed a self-healable and flexible sensing platform based on functionalized gold nanoparticle films that can be used for sensing pressure variation as well as 11 kinds of VOCs.[222] Lorwongtragool *et al.* demonstrated a novel wearable electronic nose based on flexible printed CNTs/polymer sensor array for monitoring of armpit odor (Fig. 11f).[223] This e-nose based sensor was fabricated on a polyethylene naphthalate (PEN) substrate through a low cost and scalable inject-printing technique. Both composite-like layer and composite film of MWCNTs/polymer were used as the sensing layers. The sensor was designed as a compact armband and showed feasibility to detect VOCs (*e.g.* ammonia, acetic acid, acetone and ethanol) released from the armpit regions of the human body.

Despite recent advances on breath sensing, challenges still exist in many aspects. Inherent breath confounders (*i.e.* contamination from ambient air, interference from humidity, ingested materials, *etc.*) are difficult to eliminate from breath collection and analysis. Sensing of biomarkers in gas is significantly influenced by humidity. Exposure to water vapor will induce decreased resistance of n-type oxide semiconductors and thus affect the gas-triggered response. To resolve humidity

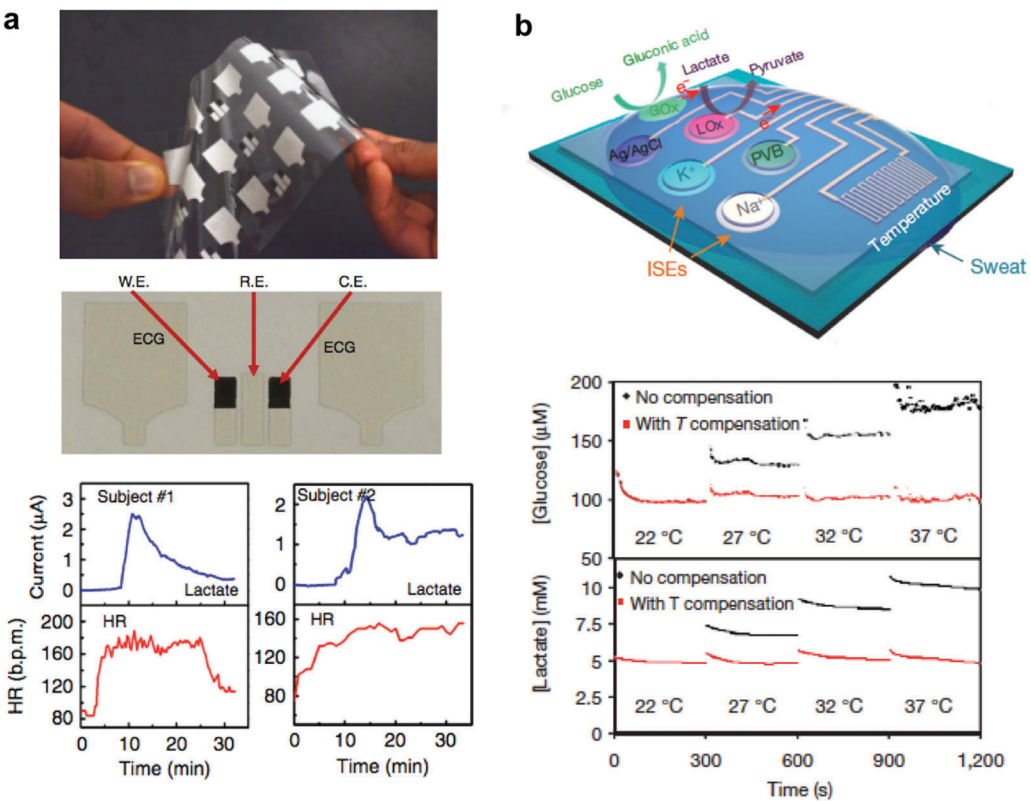

Fig. 12 Fusion of wearable and flexible physical and chemical sensors. (a) Electrocardiogram sensing integrated with lactate sensing. Exercising subject testing yields reasonable correlation between lactate levels and heart rate profile. Reproduced with permission from ref. 224. Copyright 2016 Nature Publishing Group. (b) Temperature sensing integrated with multi-analyte sensing. Temperature compensation improved the consistency of lactate and glucose measurement at different temperatures. Reproduced with permission from ref. 55. Copyright 2016 Nature Publishing Group.

interference, dehydration *via* increased sensor temperature might be considered; humidity absorbing materials such as NiO may be used to separate water molecules from the target analyte sensor, and regeneration of such absorbers is needed for continuous monitoring.[224] The devices developed were mostly tested in a controlled environment with low air disturbance, which is less realistic compared to a real-life situation. Future wearable devices should be able to accommodate different ambient conditions including temperature, humidity, and airflow. Lastly, full device integration for *in situ* real-time wireless monitoring was not yet accomplished in many wearable breath sensors. Continuous monitoring for diseases such as asthma will require a fully integrated flexible device with wireless readout and steady yet wearable power supply. In addition to the challenges described above, the concept of electronic nose could be expanded to biofluid analysis, combinatorial analysis of gas and biofluids, or among different biofluids. This concept may benefit disease classification in a broader spectrum than simply gas-based classification.

3.8. Fusion of physical and chemical sensors

Aside from wearable sensors based solely on chemical sensing principles, various wearable sensors fused both physical and chemical sensing onto a single platform. Such physical parameters include body temperature, pressure, strain, and heart rate. The implementation of these physical parameters, in addition to chemical parameters, can be used for more comprehensive evaluation of physical conditions such as wound healing progress,[191] diabetic ulceration,[187] *etc.* Imani *et al.* integrated electrocardiogram with lactate sensing on a thin, flexible polyester patch (Fig. 12a).[224] The patch consists of a screen-printed three-electrode amperometric lactate sensor and two electro-cardiogram electrodes, which enabled simultaneous measurement of sweat lactate and an electrocardiogram in real time. The device was placed on the chests of exercising human subjects and recorded sweat lactate concentration and heart rate in real time.

The measured physical parameters can also be used to calibrate chemical sensing results.[55,56] For instance, enzyme activity usually varies with temperature, and enzyme-based chemical sensors can be strongly affected by temperature variation in real-life applications. The use of temperature measurement to calibrate chemical sensing results aids in the consistency in sensor performance over time. The flexible sensor that Gao *et al.* developed incorporated physical based temperature monitoring with electrochemical detection of ions and metabolites (Fig. 12b).[55] As the temperature increases from 22 °C to 40 °C, an increase in GOx and LOx activity was observed which led to overestimation of actual glucose and lactate concentration. With the real time temperature sensing and compensation, accurate and consistent readings of glucose and lactate concentration were achieved.

4. Conclusions and outlook

In this review, we have summarized and highlighted recent advances in wearable flexible chemical sensors toward continuous health monitoring. These include wearable chemical sensors for non-invasive biomarker analysis in tears, saliva, sweat, ISF and blood, as well as sensors that can detect the gas molecules from exhaled breath. Unlike most previously reported wearable sensors that mainly tracked physical activities and vital signs, the new generation of wearable chemical sensors enable real-time and fast detection of accessible biomarkers from the human body, and allow for collection of large-scale information about the individual's dynamic health status at the molecular level. A number of key features have been identified as the advantages of the development of the wearable chemical sensors: flexibility, stretchability, biocompatibility, low-cost production and real-time continuous monitoring. These new non-invasive wearable and flexible chemical sensors have promising prospects in a variety of healthcare fields. A key example is that they provide low-cost solutions for early diagnosis, real-time in-home monitoring and management of chronic diseases. The affordable wireless health-monitoring devices will also lead to major improvements in patient monitoring, particularly for the developing countries or rural areas where the medical resources are limited, unavailable, expensive, and ineffective.

Despite significant progress made in the past few years in the field of wearable and flexible chemical sensors toward continuous health monitoring, there are many key challenges to address and technological gaps to bridge before realizing the full potential of wearable chemical sensors. One major problem is that, the amount of available wearable chemical sensors that can accurately, reliably and continuously analyze the broad spectrum of the body biomarkers is still very limited. Recently developed wearable chemical sensors mainly focus on monitoring major metabolites and electrolytes in body fluids. Most of these sensors still require further optimization in sensor stability and assessment in human trials before exploitation and routine use can happen. In addition, there are few reports on wearable devices that can monitor peptides, hormones, proteins, and DNAs/RNAs in body fluids or in exhaled breath. In fact, sweat, saliva, tears and exhaled breath contain a wealth of such analytes in trace amounts, many of which are reported to have good correlations with blood analytes or close relations with various health conditions and diseases. Continuous monitoring of these biomarkers through wearable devices would provide insightful information for screening and early diagnosis of a broad range of major health conditions. However, one of the challenges lies in the detection of the extremely low concentrations of these biomarkers in body fluids. Developing highly sensitive and selective sensors with proper pre-concentration techniques is one method of tackling this problem. Moreover, current protein or DNA sensors usually require multi-step preparation protocols with long waiting time and additional washing steps, which are not desirable for continuous wearable monitoring. Next-generation wearable chemical sensors must explore novel materials and detection techniques to target these challenging biomarkers to further expand the reach of wearable sensing technology for non-invasive, personalized health monitoring. Considering the complex physiological process of the human body, multiplexed chemical sensing or fusion of sensors for physical and chemical analysis could be extremely important to obtain accurate and insightful physiological information.

Although wearable sensing has achieved great advances in the past few years, several key milestones are yet to be reached. One of the milestones is powering the wearable devices. The tremendous progress in wearable biosensing and the increasing need for multi-tasking (sensing, processing, and communication) on wearable platforms have urged the development of efficient and sustainable power sources. For non-invasive skin-worn wearable devices, the power sources must also be flexible and stretchable to comply with skin contour and cope with mechanical stress. To this end, flexible solar cells, piezoelectric devices, thermoelectric devices, and wearable batteries were constructed in the past as abiotic energy sources.[225–227] In addition, recent studies have cast light on wearable electrochemical biofuel cells energy harvesting from biotic sources and showed the great potential of biofuel cells for wearable applications. Though the biocompatibility and auto-power features of biotic energy sources have made biofuel cells a great candidate for wearable applications, the long-term stability of the enzymes and redox mediator (if present) need to be improved for proper function of the biofuel cell. Stabilization of the enzymes should be considered and could possibly be achieved by engineering modified enzymes,[228] by applying enzyme stabilizers[229] or using better enzyme immobilization methods.[230] Although great efforts have been invested in non-invasive flexible fuel cells and biofuel cells, the current power is generally insufficient to power many current wearable electronic devices. In addition to increasing the power output of such flexible fuel cell, an alternative is to create miniaturized sensing devices with lower power consumption; using multi-source energy harvest may be also promising.

Another milestone for many wearable sensing devices lies in data processing and seamless system-level integration. In order to acquire interpretable results from wearable sensing devices, the electrical signals from sensors need to be properly processed and then transmitted for analysis and display. The electrical signals need to be converted into recordable values and sampled by the processor. Raw data sampled can be susceptible to inherent or ambient noises, and signal processing reduces these noise effects to extract useful signals from sensors. Transmission of the processed data to an external platform can allow for display and analysis of the processed data. In many cases, mathematical manipulation (*i.e.* difference between electrical potentials, rate-time profile) that requires specific analytics or even algorithm is needed to gain interpretable results corresponding to the parameter of interest. The main function of processing is noise reduction in the recorded data, but researchers have recently incorporated mathematical calculation and digital processing into the on-board platform.[231] For applications that require large data storage and complex computation, processed data need to be transmitted to a computing device (*i.e.* mobile phone, computer). Although wired connection remains an option, it imposes inconvenience on users and thus not desirable in the final device layout. At present, bluetooth low energy (BLE) and near-field communication (NFC) have been widely used in wearable sensor platforms and allow for real-time data streaming and analysis. However, BLE can be a huge drain for power supply, and NFC requires close proximity with receiver electronics. In addition to respective constraints, both technologies are not suitable for high-density data transmission, where several users have multiple sensors interacting with receivers at a high sampling rate. A transmission that fulfills ideal connectivity is yet to be developed. The analytics after signal transmission should also be carefully designed to convey relevant, useful and interpretable information to users. This will require development of efficient algorithms and user-friendly display platforms. The remote storage and processing of these personal data introduce concerns about data security and user privacy, and intensive research efforts have been made on cryptologic algorithms.[54,231]

The wearable sensing technology will not be realized without efficient commercialization. To date, most current commercial effort on wearable sensing devices has been devoted to the adaptation of current sensing methods through system miniaturization and conformal design. There is still a lack of wearable sensing products for molecular monitoring in the commercial market, due to issues such as sensor stability, biofouling and sensor degradation over time. Therefore, future commercial products may require strategies for easy replacement of sensing components (*e.g.* disposable and low cost chemical sensors) with reusable electronics components. Although there are still no commercially available wearable chemical sensors for continuous monitoring of human sweat, tears, interstitial fluids or saliva, a number of start-up companies such as Eccrine Systems (sweat monitoring), Kenzen (sweat monitoring) and MouthSense (saliva monitoring) are receiving increased attention and investment. As the interest grows, more endeavors from both research and clinical fields will help identify strategies to resolve the current limitations and issues related to chemical sensors. It is expected that the commercial wearable chemical monitor will be available to the customers within the next decade.

Although current research efforts on wearable chemical sensing technology primarily focus on developing reliable wearable and flexible chemical sensing systems, as the technologies move forward, understanding the physiological relevance of biomarkers in body fluids and exhaled breath to determine their utility for non-invasive health monitoring will be the main bottleneck to be addressed toward a broader use of wearable chemical sensors. To this end, accumulation of large sets of data across longitudinal and cohort studies can help to investigate the potential correlations and generate possible predictive algorithms. These studies present a key challenge to sweat sensor technology development in the immediate future and would require the close collaboration among engineers, scientists as well as clinicians. An attractive long-term vision of wearable devices is to heterogeneously integrate a wide range of sensor networks (*e.g.* biomolecules, vital signs) on small wearable patches that can continuously and non-invasively monitor the user's health. Big data analytics and machine learning tools can be used towards parsing the vast time series of multiplexed sensor data from these population studies to identify subtle patterns and correlations. The resulting system, coupled with the big data mined from this technology, will supplant traditional reactive, episodic healthcare with predictive and proactive diagnostics. Such technology can pave the way for future development in

wearable sensors for personalized, real time health analysis. In certain cases, upon further investigation and development, such non-invasive wearable electrochemical sensors can potentially be used as a counterpart to blood testing not only for patients in medical applications but also for the general public in daily life. Through cohort studies using the technology development of wearable and flexible electronics for continuous molecular analysis, we expect that the large sets of data and health information collected using wearable sensors from individuals' daily activities will ultimately generate predictive algorithms and revolutionize the traditional healthcare setting.

Conflicts of interest

There are no conflicts to declare.

Acknowledgements

This work is supported by the California Institute of Technology.

References

1 M. A. Hamburg and F. S. Collins, *N. Engl. J. Med.*, 2010, **363**, 301–304.
2 J. Larry Jameson and D. L. Longo, *Obstet. Gynecol. Surv.*, 2015, **70**, 612–614.
3 J. Gubbi, R. Buyya, S. Marusic and M. Palaniswami, *Future Gener. Comput. Syst.*, 2013, **29**, 1645–1660.
4 M. Hassanalieragh, A. Page, T. Soyata, G. Sharma, M. Aktas, G. Mateos, B. Kantarci and S. Andreescu, *Proc. IEEE Int. Conf. Serv. Comput.*, 2015, 285–292.
5 S. Patel, H. Park, P. Bonato, L. Chan and M. A. Rodgers, *J. NeuroEng. Rehabil.*, 2012, **9**, 1–17.
6 S. C. Mukhopadhyay, *IEEE Sens.*, 2015, **15**, 1321–1330.
7 M. Stoppa and A. Chiolerio, *Sensors*, 2014, **14**, 11957–11992.
8 D.-H. Kim, R. Ghaffari, N. Lu and J. A. Rogers, *Annu. Rev. Biomed. Eng.*, 2012, **14**, 113–128.
9 D.-H. Kim, N. Lu, R. Ma, Y. Kim, R. Kim, S. Wang, J. Wu, S. M. Won, H. Tao, A. Islam, K. J. Yu, T. Kim, R. Chowdhury, M. Ying, L. Xu, M. Li, H.-J. Chung, H. Keum, M. McCormick, P. Liu, Y. Zhang, F. G. Omenetto, Y. Huang, T. Coleman and J. A. Rogers, *Science*, 2011, **333**, 838–843.
10 M. L. Hammock, A. Chortos, B. C. K. Tee, J. B. H. Tok and Z. Bao, *Adv. Mater.*, 2013, **25**, 5997–6038.
11 J.-Y. Sun, X. Zhao, W. R. K. Illeperuma, O. Chaudhuri, K. H. Oh, D. J. Mooney, J. J. Vlassak and Z. Suo, *Nature*, 2012, **489**, 133–136.
12 J. A. Rogers, T. Someya and Y. Huang, *Science*, 2010, **327**, 1603–1607.
13 M. Kaltenbrunner, T. Sekitani, J. Reeder, T. Yokota, K. Kuribara, T. Tokuhara, M. Drack, R. Schwödiauer, I. Graz, S. Bauer-Gogonea, S. Bauer and T. Someya, *Nature*, 2013, **499**, 458–463.
14 A. M. Hussain and M. M. Hussain, *Adv. Mater.*, 2016, **28**, 4219–4249.
15 S. Choi, H. Lee, R. Ghaffari, T. Hyeon and D.-H. Kim, *Adv. Mater.*, 2016, **28**, 4203–4218.
16 K. Chen, W. Gao, S. Emaminejad, D. Kiriya, H. Ota, H. Y. Nyein, K. Takei and A. Javey, *Adv. Mater.*, 2016, **28**, 4397–4414.
17 M. Amjadi, A. Pichitpajongkit, S. Lee, S. Ryu and I. Park, *ACS Nano*, 2014, **8**, 5154–5163.
18 C. Pang, C. Lee and K. Y. Suh, *J. Appl. Polym. Sci.*, 2013, **130**, 1429–1441.
19 D. J. Lipomi, M. Vosgueritchian, B. C.-K. Tee, S. L. Hellstrom, J. A. Lee, C. H. Fox and Z. Bao, *Nat. Nanotechnol.*, 2011, **6**, 788–792.
20 Y. Gao, H. Ota, E. W. Schaler, K. Chen, A. Zhao, W. Gao, H. M. Fahad, Y. Leng, A. Zheng, F. Xiong, C. Zhang, L.-C. Tai, P. Zhao, R. S. Fearing and A. Javey, *Adv. Mater.*, 2017, **29**, 1701985.
21 B. Nie, R. Li, J. Cao, J. D. Brandt and T. Pan, *Adv. Mater.*, 2015, **27**, 6055–6062.
22 L. Pan, A. Chortos, G. Yu, Y. Wang, S. Isaacson, R. Allen, Y. Shi, R. Dauskardt and Z. Bao, *Nat. Commun.*, 2014, **5**, 3002.
23 J. Lee, H. Kwon, J. Seo, S. Shin, J. H. Koo, C. Pang, S. Son, J. H. Kim, Y. H. Jang, D. E. Kim and T. Lee, *Adv. Mater.*, 2015, **27**, 2433–2439.
24 C. Wang, D. Hwang, Z. Yu, K. Takei, J. Park, T. Chen, B. Ma and A. Javey, *Nat. Mater.*, 2013, **12**, 899–904.
25 K. Takei, T. Takahashi, J. C. Ho, H. Ko, A. G. Gillies, P. W. Leu, R. S. Fearing and A. Javey, *Nat. Mater.*, 2010, **9**, 821.
26 Z. Wen, M. H. Yeh, H. Guo, J. Wang, Y. Zi, W. Xu, J. Deng, L. Zhu, X. Wang, C. Hu, L. Zhu, X. Sun and Z. L. Wang, *Sci. Adv.*, 2016, **2**, e1600097.
27 H. Wang, P. Hu, J. Yang, G. Gong, L. Guo and X. Chen, *Adv. Mater.*, 2015, **27**, 2348–2354.
28 S. P. Lacour, G. Courtine and J. Guck, *Nat. Rev. Mater.*, 2016, **1**, 16063.
29 T. Q. Trung and N.-E. Lee, *Adv. Mater.*, 2016, **28**, 4338–4372.
30 Y. Khan, A. E. Ostfeld, C. M. Lochner, A. Pierre and A. C. Arias, *Adv. Mater.*, 2016, **28**, 4373–4395.
31 A. Chortos, J. Liu and Z. Bao, *Nat. Mater.*, 2016, **15**, 937–950.
32 G. Schwartz, B. C. Tee, J. Mei, A. L. Appleton, D. H. Kim, H. Wang and Z. Bao, *Nat. Commun.*, 2013, **4**, 1859.
33 S. Y. Kim, S. Park, H. W. Park, D. H. Park, Y. Jeong and D.-H. Kim, *Adv. Mater.*, 2015, **27**, 4178–4185.
34 J. Y. Sun, C. Keplinger, G. M. Whitesides and Z. Suo, *Adv. Mater.*, 2014, **26**, 7608–7614.
35 C. Dagdeviren, Y. Su, P. Joe, R. Yona, Y. Liu, Y. S. Kim, Y. Huang, A. R. Damadoran, J. Xia, L. W. Martin, Y. Huang and J. A. Rogers, *Nat. Commun.*, 2014, **5**, 4496.
36 X. W. Wang, Y. Gu, Z. P. Xiong, C. Zheng and T. Zhang, *Adv. Mater.*, 2014, **26**, 1336–1342.
37 B. Xu, A. Akhtar, Y. Liu, H. Chen, W. H. Yeo, S. I. Park, B. Boyce, H. Kim, J. Yu, H. Y. Lai, S. Jung, Y. Zhou, J. Kim, S. Cho, Y. Huang, T. Bretl and J. A. Rogers, *Adv. Mater.*, 2016, **28**, 4462–4471.

38 B. Zhu, Z. Niu, H. Wang, W. R. Leow, H. Wang, Y. Li, L. Zheng, J. Wei, F. Huo and X. Chen, *Small*, 2014, **10**, 3625–3631.

39 S. Xu, Y. Zhang, L. Jia, K. E. Mathewson, K.-I. Jang, J. Kim, H. Fu, X. Huang, P. Chava, R. Wang, S. Bhole, L. Wang, Y. J. Na, Y. Guan, M. Flavin, Z. Han, Y. Huang and J. A. Rogers, *Science*, 2014, **344**, 70–74.

40 R. C. Webb, Y. Ma, S. Krishnan, Y. Li, S. Yoon, X. Guo, X. Feng, Y. Shi, M. Seidel, N. H. Cho, J. Kurniawan, J. Ahad, N. Sheth, J. Kim, J. G. Taylor, J. T. Darlington, K. Chang, W. Huang, J. Ayers and A. Gruebele, *Sci. Adv.*, 2015, **1**, e1500701.

41 D.-H. Kim, N. Lu, R. Ghaffari, Y.-S. Kim, S. P. Lee, L. Xu, J. Wu, R.-H. Kim, J. Song, Z. Liu, J. Viventi, B. de Graff, B. Elolampi, M. Mansour, M. J. Slepian, S. Hwang, J. D. Moss, S. M. Won, Y. Huang, B. Litt and J. A. Rogers, *Nat. Mater.*, 2011, **10**, 316–323.

42 Y. Liu, J. J. Norton, R. Qazi, Z. Zou, K. R. Ammann, H. Liu, L. Yan, P. L. Tran, K.-I. Jang, J. W. Lee, D. Zhang, K. A. Kilian, S. H. Jung, T. Bretl, J. Xiao, M. J. Slepian, Y. Huang, J.-W. Jeong and J. A. Rogers, *Sci. Adv.*, 2016, **2**, e1601185.

43 Y. Liu, M. Pharr and G. A. Salvatore, *ACS Nano*, 2017, **11**, 9614–9635.

44 Y. S. Rim, S.-H. Bae, H. Chen, N. D. Marco and Y. Yang, *Adv. Mater.*, 2016, **28**, 4415–4440.

45 T. Q. Trung and N.-E. Lee, *Adv. Mater.*, 2016, **28**, 4338–4372.

46 M. Gao, L. Li and Y. Song, *J. Mater. Chem. C*, 2017, **5**, 2971–2993.

47 J. S. Heo, J. Eom, Y.-H. Kim and S. K. Park, *Small*, 2017, **14**, 1703034.

48 A. Nag, S. C. Mukhopadhyay and J. Kosel, *IEEE Sens. J.*, 2017, **17**, 3949–3960.

49 A. J. Atkinson, W. A. Colburn, V. G. DeGruttola, D. L. DeMets, G. J. Downing, D. F. Hoth, J. A. Oates, C. C. Peck, R. T. Schooley and B. A. Spilker, *Clin. Pharmacol. Ther.*, 2001, **69**, 89–95.

50 K. Strimbu and J. A. Tavel, *Curr. Opin. HIV AIDS*, 2010, **5**, 463–466.

51 A. Hulanicki, S. Glab and F. Ingman, *Pure Appl. Chem.*, 1991, **63**, 1247–1250.

52 A. J. Bandodkar and J. Wang, *Trends Biotechnol.*, 2014, **32**, 363–371.

53 G. Matzeu, L. Florea and D. Diamond, *Sens. Actuators, B*, 2015, **211**, 403–418.

54 A. J. Bandodkar, I. Jeerapan and J. Wang, *ACS Sens.*, 2016, **1**, 464–482.

55 W. Gao, S. Emaminejad, H. Y. Nyein, S. Challa, K. Chen, A. Peck, H. M. Fahad, H. Ota, H. Shiraki, D. Kiriya, D. H. Lien, G. A. Brooks, R. W. Davis and A. Javey, *Nature*, 2016, **529**, 509–514.

56 H. Lee, T. K. Choi, Y. B. Lee, H. R. Cho, R. Ghaffari, L. Wang, H. J. Choi, T. D. Chung, N. Lu, T. Hyeon, S. H. Choi and D.-H. Kim, *Nat. Nanotechnol.*, 2016, **11**, 566–572.

57 A. Koh, D. Kang, Y. Xue, S. Lee, R. M. Pielak, J. Kim, T. Hwang, S. Min, A. Banks, P. Bastien, M. C. Manco, L. Wang, K. R. Ammann, K.-I. Jang, P. Won, S. Han, R. Ghaffari, U. Paik, M. J. Slepian, G. Balooch, Y. Huang and J. A. Rogers, *Sci. Transl. Med.*, 2016, **8**, 366ra165.

58 J. Wang, *Analytical Electrochemisitry: Controlled-Potential Techniques*, John Wiley/Sons, Hoboken, 2006.

59 E. Bakker, P. Bühlmann and E. Pretsch, *Chem. Rev.*, 1997, **97**, 3083–3132.

60 C. McDonagh, C. S. Burke and B. D. MacCraith, *Chem. Rev.*, 2008, **108**, 400–422.

61 S. Coyle, V. F. Curto, F. Benito-Lopez, L. Florea and D. Diamond, *Wearable Sensors*, 2014, pp. 65–83.

62 S. Coyle, F. Benito-Lopez, R. Byrne and D. Diamond, *Wearable and Autonomous Biomedical Devices and Systems for Smart Environment, Lecture Notes in Electrical Engineering*, 2010, pp. 177–193.

63 D. Diamond, S. Coyle, S. Scarmagnani and J. Hayes, *Chem. Rev.*, 2008, **108**, 652–679.

64 M. Bariya, H. Y. Y. Nyein and A. Javey, *Nature Electron.*, 2018, **1**, 160–171.

65 K. Mitsubayashi, M. Suzuki, E. Tamiya and I. Karube, *Anal. Chim. Acta*, 1994, **289**, 27–34.

66 K. Wilke, A. Martin, L. Terstegen and S. S. Biel, *Int. J. Cosmet. Sci.*, 2007, **29**, 169–179.

67 K. Sato, W. Kang, K. Saga and K. Sato, *J. Am. Acad. Dermatol.*, 1989, **20**, 537–563.

68 Z. Sonner, E. Wilder, J. Heikenfeld, G. Kasting, F. Beyette, D. Swaile, F. Sherman, J. Joyce, J. Hagen, N. Kelley-Loughnane and R. Naik, *Biomicrofluidics*, 2015, **9**, 031301.

69 M. J. Buono, *Exp. Physiol.*, 1999, **84**, 401–404.

70 T. Kamei, T. Tsuda, Y. Mibu, S. Kitagawa, H. Wada, K. Naitoh and K. Nakashima, *Anal. Chim. Acta*, 1998, **365**, 259–266.

71 R. Keller and J. Sands, *FASEB J.*, 2014, **28**, LB719.

72 Y. Y. Al-Tamer, E. A. Hadi and I. E. I. Al-Badrani, *Urol. Res.*, 1997, **25**, 337–340.

73 K. Sato, *Rev. Physiol., Biochem. Pharmacol.*, 1977, **79**, 51–131.

74 B. P. O'Sullivan and S. D. Freedman, *Lancet*, 2009, **373**, 1891–1904.

75 W. Jia, A. J. Bandodkar, G. Valdés-Ramírez, J. R. Windmiller, Z. Yang, J. Ramírez, G. Chan and J. Wang, *Anal. Chem.*, 2013, **85**, 6553–6560.

76 A. J. Bandodkar, V. W. S. Hung, W. Jia, G. Valdés-Ramírez, J. R. Windmiller, A. G. Martinez, J. Ramírez, G. Chan, K. Kerman and J. Wang, *Analyst*, 2013, **138**, 123–128.

77 J. Kim, W. R. de Araujo, I. A. Samek, A. J. Bandodkar, W. Jia, B. Brunetti, T. R. L. C. Paixão and J. Wang, *Electrochem. Commun.*, 2015, **51**, 41–45.

78 T. Guinovart, A. J. Bandodkar, J. R. Windmiller, F. J. Andrade and J. Wang, *Analyst*, 2013, **138**, 7031.

79 J. Kim, I. Jeerapan, S. Imani, T. N. Cho, A. Bandodkar, S. Cinti, P. P. Mercier and J. Wang, *ACS Sens.*, 2016, **1**, 1011–1019.

80 A. J. Bandodkar, D. Molinnus, O. Mirza, T. Guinovart, J. R. Windmiller, G. Valdés-Ramírez, F. J. Andrade, M. J. Schöning and J. Wang, *Biosens. Bioelectron.*, 2014, **54**, 603–609.

81 D. P. Rose, M. E. Ratterman, D. K. Griffin, L. Hou, N. Kelley-Loughnane, R. R. Naik, J. A. Hagen, I. Papautsky and J. C. Heikenfeld, *IEEE Trans. Biomed. Eng.*, 2015, **62**, 1457–1465.

82 H. Y. Y. Nyein, W. Gao, Z. Shahpar, S. Emaminejad, S. Challa, K. Chen, H. M. Fahad, L.-C. Tai, H. Ota, R. W. Davis and A. Javey, *ACS Nano*, 2016, **10**, 7216–7224.

83 W. Gao, H. Y. Y. Nyein, Z. Shahpar, H. M. Fahad, K. Chen, S. Emaminejad, Y. Gao, L.-C. Tai, H. Ota, E. Wu, J. Bullock, Y. Zeng, D.-H. Lien and A. Javey, *ACS Sens.*, 2016, **1**, 866–874.

84 H. Lee, T. K. Choi, Y. B. Lee, H. R. Cho, R. Ghaffari, L. Wang, H. J. Choi, T. D. Chung, N. Lu, T. Hyeon, S. H. Choi and D.-H. Kim, *Nat. Nanotechnol.*, 2016, **11**, 566–572.

85 S. Nakata, T. Arie, S. Akita and K. Takei, *ACS Sens.*, 2017, **2**, 443–448.

86 X. Huang, Y. Liu, K. Chen, W.-J. Shin, C.-J. Lu, G.-W. Kong, D. Patnaik, S.-H. Lee, J. F. Cortes and J. A. Rogers, *Small*, 2014, **10**, 3083–3090.

87 V. F. Curto, C. Fay, S. Coyle, R. Byrne, C. O'Toole, C. Barry, S. Hughes, N. Moyna, D. Diamond and F. Benito-Lopez, *Sens. Actuators, B*, 2012, **171–172**, 1327–1334.

88 S. Emaminejad, W. Gao, E. Wu, Z. A. Davies, H. Y. Y. Nyein, S. Challa, S. P. Ryan, H. M. Fahad, K. Chen, Z. Shahpar, S. Talebi, C. Milla, A. Javey and R. W. Davis, *Proc. Natl. Acad. Sci. U. S. A.*, 2017, **114**, 4625–4630.

89 A. Martín, J. Kim, J. F. Kurniawan, J. R. Sempionatto, J. R. Moreto, G. Tang, A. S. Campbell, A. Shin, M. Y. Lee, X. Liu and J. Wang, *ACS Sens.*, 2017, **2**, 1860–1868.

90 D. Morris, S. Coyle, Y. Wu, K. T. Lau, G. Wallace and D. Diamond, *Sens. Actuators, B*, 2009, **139**, 231–236.

91 B. Schazmann, D. Morris, C. Slater, S. Beirne, C. Fay, R. Reuveny, N. Moyna and D. Diamond, *Anal. Methods*, 2010, **2**, 342–348.

92 S. Coyle, K.-T. Lau, N. Moyna, D. O'Gorman, D. Diamond, F. Di Francesco, D. Costanzo, P. Salvo, M. G. Trivella, D. E. De Rossi, N. Taccini, R. Paradiso, J.-A. Porchet, A. Ridolfi, J. Luprano, C. Chuzel, T. Lanier, F. Revol-Cavalier, S. Schoumacker, V. Mourier, I. Chartier, R. Convert, H. De-Moncuit and C. Bini, *IEEE Trans. Inf. Technol. Biomed.*, 2010, **14**, 364–370.

93 A. P. Selvam, S. Muthukumar, V. Kamakoti and S. Prasad, *Sci. Rep.*, 2016, **6**, 23111.

94 D.-H. Choi, J. S. Kim, G. R. Cutting and P. C. Searson, *Anal. Chem.*, 2016, **88**, 12241–12247.

95 Z. Sonner, E. Wilder, T. Gaillard, G. Kasting and J. Heikenfeld, *Lab Chip*, 2017, **17**, 2550–2560.

96 R. D. Munje, S. Muthukumar and S. Prasad, *Sens. Actuators, B*, 2017, **238**, 482–490.

97 S. Wang, Y. Wu, Y. Gu, T. Li, H. Luo, L.-H. Li, Y. Bai, L. Li, L. Liu, Y. Cao, H. Ding and T. Zhang, *Anal. Chem.*, 2017, **89**, 10224–10231.

98 N. Coppedè, G. Tarabella, M. Villani, D. Calestani, S. Iannotta and A. Zappettini, *J. Mater. Chem. B*, 2014, **2**, 5620–5626.

99 E. L. Tur-García, F. Davis, S. D. Collyer, J. L. Holmes, H. Barr and S. P. J. Higson, *Sens. Actuators, B*, 2017, **242**, 502–510.

100 W. Han, H. He, L. Zhang, C. Dong, H. Zeng, Y. Dai, L. Xing, Y. Zhang and X. Xue, *ACS Appl. Mater. Interfaces*, 2017, **9**, 29526–29537.

101 J. R. Sempionatto, T. Nakagawa, A. Pavinatto, S. T. Mensah, S. Imani, P. Mercier and J. Wang, *Lab Chip*, 2017, **17**, 1834–1842.

102 J. B. Sloan and K. Soltani, *J. Am. Acad. Dermatol.*, 1986, **15**, 671–684.

103 R. Peng, Z. Sonner, A. Hauke, E. Wilder, J. Kasting, T. Gaillard, D. Swaille, F. Sherman, X. Mao, J. Hagen, R. Murdock and J. Heikenfeld, *Lab Chip*, 2016, **16**, 4415–4423.

104 J. Choi, D. Kang, S. Han, S. B. Kim and J. A. Rogers, *Adv. Healthcare Mater.*, 2017, **6**, 1601355.

105 J. Choi, Y. Xue, W. Xia, T. R. Ray, J. T. Reeder, A. J. Bandodkar, D. Kang, S. Xu, Y. Huang and J. A. Rogers, *Lab Chip*, 2017, **17**, 2572–2580.

106 I. Jalbert, *Exp. Eye Res.*, 2013, **117**, 138–146.

107 F. J. Holly and M. A. Lemp, *Surv. Ophthalmol.*, 1977, **22**, 69–87.

108 N. von Thun und Hohenstein-Blaul, S. Funke and F. H. Grus, *Exp. Eye Res.*, 2013, **117**, 126–137.

109 D. K. Sen and G. S. Sarin, *Br. J. Ophthalmol.*, 1980, **64**, 693–695.

110 J. T. Baca, D. N. Finegold and S. A. Asher, *Ocul. Surf.*, 2007, **5**, 280–293.

111 H. Kudo, T. Sawada, E. Kazawa, H. Yoshida, Y. Iwasaki and K. Mitsubayashi, *Biosens. Bioelectron.*, 2006, **22**, 558–562.

112 S. Iguchi, H. Kudo, T. Saito, M. Ogawa, H. Saito, K. Otsuka, A. Funakubo and K. Mitsubayashi, *Biomed. Microdevices*, 2007, **9**, 603–609.

113 M. X. Chu, K. Miyajima, D. Takahashi, T. Arakawa, K. Sano, S. Sawada, H. Kudo, Y. Iwasaki, K. Akiyoshi, M. Mochizuki and K. Mitsubayashi, *Talanta*, 2011, **83**, 960–965.

114 H. Yao, A. J. Shum, M. Cowan, I. Lähdesmäki and B. A. Parviz, *Bios. Bioelectron.*, 2011, **26**, 3290–3296.

115 Y. T. Liao, H. Yao, A. Lingley, B. Parviz and B. P. Otis, *IEEE J. Solid-State Circuits*, 2012, **47**, 335–344.

116 J. Kim, M. Kim, M.-S. Lee, K. Kim, S. Ji, Y.-T. Kim, J. Park, K. Na, K.-H. Bae, H. K. Kim, F. Bien, C. Y. Lee and J.-U. Park, *Nat. Commun.*, 2017, **8**, 14997.

117 J. Zhang, W. Hodge, C. Hutnick and X. Wang, *J. Diabetes Sci. Technol.*, 2011, **5**, 166–172.

118 R. Badugu, J. R. Lakowicz and C. D. Geddes, *Analyst*, 2004, **129**, 516–521.

119 J.-L. Ruan, C. Chen, J.-H. Shen, X.-L. Zhao, S.-H. Qian and Z.-G. Zhu, *Polymers*, 2017, **9**, 125.

120 K. Dumbleton, *Contact Lens Anterior Eye*, 2002, **25**, 137–146.

121 M. A. Javaid, A. S. Ahmed, R. Durand and S. D. Tran, *J. Oral Biol. Craniofacial Res.*, 2016, **6**, 67–76.

122 Y. Goswami, R. Mishra, A. Agrawal and L. Agrawal, *J. Dent. Med. Sci.*, 2015, **14**, 80–87.

123 R. S. P. Malon, S. Sadir, M. Balakrishnan and E. P. Córcoles, *BioMed Res. Int.*, 2014, **2014**, 1–20.

124 U. M. Nater and N. Rohleder, *Psychoneuroendocrinology*, 2009, **34**, 486–496.

125 A. van Stegeren, N. Rohleder, W. Everaerd and O. T. Wolf, *Psychoneuroendocrinology*, 2006, **31**, 137–141.
126 M. V. Thoma, C. Kirschbaum, J. M. Wolf and N. Rohleder, *Biol. Psychol.*, 2012, **91**, 342–348.
127 T. F. Oberlander, J. Weinberg, M. Papsdorf, R. Grunau, S. Misri and A. M. Devlin, *Epigenetics*, 2008, **3**, 97–106.
128 H. M. Burke, M. C. Davis, C. Otte and D. C. Mohr, *Psychoneuroendocrinology*, 2005, **30**, 846–856.
129 M. Castro, P. C. L. Elias, C. E. Martinelli Jr., S. R. R. Antonini, L. Santiago and A. C. Moreira, *Braz. J. Med. Biol. Res.*, 2000, **33**, 1171–1175.
130 I.-H. Kim, C. Kim, K. Seong, M.-H. Hur, H. M. Lim and M. S. Lee, *J. Evidence-Based Complementary Altern. Med.*, 2012, **2012**, 1–9.
131 K. Fransen, T. Vermoesen, G. Beelaert, J. Menten, V. Hutse, K. Wouters, T. Platteau and E. Florence, *J. Virol. Methods*, 2013, **194**, 46–51.
132 E. H. El and W. A. Arafa, *J. Egypt. Soc. Parasitol.*, 2004, **34**, 1095–1104.
133 L. R. Bigler, C. F. Streckfus, L. Copeland, R. Burns, X. Dai, M. Kuhn, P. Martin and S. A. Bigler, *J. Oral Pathol. Med.*, 2002, **31**, 421–431.
134 E.-M. Poll, I. Kreitschmann-Andermahr, Y. Langejuergen, S. Stanzel, J. M. Gilsbach, A. Gressner and E. Yagmur, *Clin. Chim. Acta*, 2007, **382**, 15–19.
135 M. Navazesh, *Ann. N. Y. Acad. Sci.*, 1993, **694**, 72–77.
136 R. C. Stevens, S. D. Soelberg, S. Near and C. E. Furlong, *Anal. Chem.*, 2008, **80**, 6747–6751.
137 W. Yantasee, C. Timchalk, K. K. Weitz, D. A. Moore and Y. Lin, *Talanta*, 2005, **67**, 617–624.
138 M. S. Mannoor, H. Tao, J. D. Clayton, A. Sengupta, D. L. Kaplan, R. R. Naik, N. Verma, F. G. Omenetto and M. C. McAlpine, *Nat. Commun.*, 2012, **3**, ncomms1767.
139 J. Kim, G. Valdés-Ramírez, A. J. Bandodkar, W. Jia, A. G. Martinez, J. Ramírez, P. Mercier and J. Wang, *Analyst*, 2014, **139**, 1632–1636.
140 J. Kim, S. Imani, W. R. de Araujo, J. Warchall, G. Valdés-Ramírez, T. R. L. C. Paixão, P. P. Mercier and J. Wang, *Biosens. Bioelectron.*, 2015, **74**, 1061–1068.
141 T. Arakawa, Y. Kuroki, H. Nitta, P. Chouhan, K. Toma, S. Sawada, S. Takeuchi, T. Sekita, K. Akiyoshi, S. Minakuchi and K. Mitsubayashi, *Biosens. Bioelectron.*, 2016, **84**, 106–111.
142 R. P. Peters, M. A. van Agtmael, S. A. Danner, P. H. Savelkoul and C. M. Vandenbroucke-Grauls, *Lancet Infect. Dis.*, 2004, **4**, 751–760.
143 M. Hallek, B. D. Cheson, D. Catovsky, F. Caligaris-Cappio, G. Dighiero, H. Döhner, P. Hillmen, M. J. Keating, E. Montserrat, K. R. Rai and T. J. Kipps, *Blood*, 2008, **111**, 5446–5456.
144 A. D. Association, *Diabetes Care*, 2014, **37**, S81–S90.
145 S. K. Garg, S. Schwartz and S. V. Edelman, *Diabetes Care*, 2004, **27**, 734–738.
146 M. S. Boyne, D. M. Silver, J. Kaplan and C. D. Saudek, *Diabetes*, 2003, **52**, 2790–2794.
147 B. Seok Lee, J.-N. Lee, J.-M. Park, J.-G. Lee, S. Kim, Y.-K. Cho and C. Ko, *Lab Chip*, 2009, **9**, 1548–1555.
148 B. Seok Lee, Y. Ui Lee, H.-S. Kim, T.-H. Kim, J. Park, J.-G. Lee, J. Kim, H. Kim, W. Gyo Lee and Y.-K. Cho, *Lab Chip*, 2011, **11**, 70–78.
149 T. Zheng, N. Pierre-Pierre, X. Yan, Q. Huo, A. J. O. Almodovar, F. Valerio, I. Rivera-Ramirez, E. Griffith, D. D. Decker, S. Chen and N. Zhu, *ACS Appl. Mater. Interfaces*, 2015, **7**, 6819–6827.
150 Y. Mendelson, *Clin. Chem.*, 1992, **38**, 1601–1607.
151 N. D. Giardino, L. Chan and S. Borson, *Appl. Psychophysiol. Biofeedback*, 2004, **29**, 121–133.
152 M. Nitzan, A. Romem and R. Koppel, *Med. Devices*, 2014, **7**, 231–239.
153 R. G. Haahr, S. B. Duun, M. H. Toft, B. Belhage, J. Larsen, K. Birkelund and E. V. Thomsen, *IEEE Trans. Biomed. Circuits Syst.*, 2012, **6**, 45–53.
154 B. Venema, N. Blanik, V. Blazek, H. Gehring, A. Opp and S. Leonhardt, *IEEE Trans. Biomed. Eng.*, 2012, **59**, 2003–2010.
155 C. M. Lochner, Y. Khan, A. Pierre and A. C. Arias, *Nat. Commun.*, 2014, **5**, 5745.
156 T. Yokota, P. Zalar, M. Kaltenbrunner, H. Jinno, N. Matsuhisa, H. Kitanosako, Y. Tachibana, W. Yukita, M. Koizumi and T. Someya, *Sci. Adv.*, 2016, **2**, e1501856.
157 J. Kim, P. Gutruf, A. M. Chiarelli, S. Y. Heo, K. Cho, Z. Xie, A. Banks, S. Han, K.-I. Jang, J. W. Lee, K.-T. Lee, X. Feng, Y. Huang, M. Fabiani, G. Gratton, U. Paik and J. A. Rogers, *Adv. Funct. Mater.*, 2017, **27**, 1604373.
158 J. M. Goldman, M. T. Petterson, R. J. Kopotic and S. J. Barker, *J. Clin. Monit. Comput.*, 2000, **16**, 475–483.
159 R. Yousefi, M. Nourani, S. Ostadabbas and I. Panahi, *IEEE J. Biomed. Health Inform.*, 2014, **18**, 670–681.
160 S. K. Vashist, *Anal. Chim. Acta*, 2012, **750**, 16–27.
161 J. Yadav, A. Rani, V. Singh and B. M. Murari, *Proc. Int. Conf. Signal Process. Integr. Netw.*, 2014, 591–594.
162 A. Mason, O. Korostynska, J. Louis, L. E. Cordova-Lopez, B. Abdullah, J. Greene, R. Connell and J. Hopkins, *IEEE Trans. Biomed. Eng.*, 2017, 1.
163 N. Fogh-Andersen, B. M. Altura, B. T. Altura and O. Siggaard-Andersen, *Clin. Chem.*, 1995, **41**, 1522–1525.
164 A. Sieg, F. Jeanneret, M. Fathi, D. Hochstrasser, S. Rudaz, J. L. Veuthey, R. H. Guy and M. B. Delgado-Charro, *Eur. J. Pharm. Biopharm.*, 2009, **72**, 226–231.
165 I. T. Degim, S. Ilbasmis, R. Dundaroz and Y. Oguz, *Pediatr. Nephrol.*, 2003, **18**, 1032–1037.
166 B. Leboulanger, R. H. Guy and M. B. Delgado-Charro, *Eur. J. Pharm. Sci.*, 2004, **22**, 427–433.
167 A. J. Bandodkar and J. Wang, *Trends Biotechnol.*, 2014, **32**, 363–371.
168 J. M. Yuen, N. C. Shah, J. T. Walsh, M. R. Glucksberg and R. P. Van Duyne, *Anal. Chem.*, 2010, **82**, 8382–8385.
169 G. Rao, P. Glikfeld and R. H. Guy, *Pharm. Res.*, 1993, **10**, 1751–1755.
170 B. Leboulanger, R. H. Guy and M. B. Delgado-Charro, *Physiol. Meas.*, 2004, **25**, R35.
171 L. J. De Groot, G. Chrousos, K. Dungan, K. R. Feingold, A. Grossman, J. M. Hershman, C. Koch, M. Korbonits, R. McLachlan, M. New, J. Purnell, R. Rebar, F. Singer and

A. Vinik, *Endotext*, MDText.com, Inc., South Dartmouth (MA), 2000.
172 S. V. Edelman, *Diabetes Technol. Ther.*, 2001, **3**, 283–284.
173 A. J. Bandodkar, W. Jia, C. Yardımcı, X. Wang, J. Ramirez and J. Wang, *Anal. Chem.*, 2015, **87**, 394–398.
174 Y. Chen, S. Lu, S. Zhang, Y. Li, Z. Qu, Y. Chen, B. Lu, X. Wang and X. Feng, *Sci. Adv.*, 2017, **3**, e1701629.
175 H. Yu, D. Li, R. C. Roberts, K. Xu and N. C. Tien, *J. Microelectromech. Syst.*, 2012, **21**, 917–925.
176 Z. Pu, R. Wang, K. Xu, D. Li and H. Yu, *IEEE Sens.*, 2015, 1–4.
177 Z. Pu, C. Zou, R. Wang, X. Lai, H. Yu, K. Xu and D. Li, *Biomicrofluidics*, 2016, **10**, 011910.
178 M. Venugopal, K. E. Feuvrel, D. Mongin, S. Bambot, M. Faupel, A. Panangadan, A. Talukder and R. Pidva, *IEEE Sens. J.*, 2008, **8**, 71–80.
179 M. Venugopal, S. K. Arya, G. Chornokur and S. Bhansali, *Sens. Actuators, A*, 2011, **172**, 154–160.
180 H. P. Lorenz and M. T. Longaker, *Surgery*, Springer, New York, NY, 2008, 191–208.
181 K. F. Cutting, *Br. J. Community Nurs.*, 2003, **8**, S4–S9.
182 R. O. Niskanen, O. Korkala and H. Pammo, *J. Bone Joint Surg. Br.*, 1996, **78**, 431–433.
183 P. Kujath and A. Michelsen, *Dtsch. Arztebl. Int.*, 2008, **105**, 239–248.
184 M. L. Fernandez, Z. Upton, H. Edwards, K. Finlayson and G. K. Shooter, *Int. Wound J.*, 2012, **9**, 139–149.
185 D. W. Edlow and W. H. Sheldon, *Proc. Soc. Exp. Biol. Med.*, 1971, **137**, 1328–1332.
186 B. Greener, A. a. Hughes, N. p. Bannister and J. Douglass, *J. Wound Care*, 2005, **14**, 59–61.
187 M. Turns, *Br. J. Nurs.*, 2011, S19–S25.
188 F. Gottrup, *Am. J. Surg.*, 2004, **187**, S38–S43.
189 T. R. Dargaville, B. L. Farrugia, J. A. Broadbent, S. Pace, Z. Upton and N. H. Voelcker, *Biosens. Bioelectron.*, 2013, **41**, 30–42.
190 S. Pasche, S. Angeloni, R. Ischer, M. Liley, J. Luprano and G. Voirin, *Adv. Sci. Technol.*, 2008, **57**, 80–87.
191 N. Mehmood, A. Hariz, S. Templeton and N. H. Voelcker, *BioMed. Eng. OnLine*, 2015, **14**, 17.
192 Y. Hattori, L. Falgout, W. Lee, S.-Y. Jung, E. Poon, J. W. Lee, I. Na, A. Geisler, D. Sadhwani, Y. Zhang, Y. Su, X. Wang, Z. Liu, J. Xia, H. Cheng, R. C. Webb, A. P. Bonifas, P. Won, J.-W. Jeong, K.-I. Jang, Y. M. Song, B. Nardone, M. Nodzenski, J. A. Fan, Y. Huang, D. P. West, A. S. Paller, M. Alam, W.-H. Yeo and J. A. Rogers, *Adv. Healthcare Mater.*, 2014, **3**, 1597–1607.
193 M. Punjiya, H. Rezaei, M. A. Zeeshan and S. Sonkusale, *Proc. IEEE Int. Conf. Solid-State Sens. Actuators Microsyst.*, 2017, 1700–1702.
194 M. Punjiya, P. Mostafalu and S. Sonkusale, *Proc. IEEE Int. Midwest Symp. Circuits Syst.*, 2017, 495–498.
195 T. Guinovart, G. Valdés-Ramírez, J. R. Windmiller, F. J. Andrade and J. Wang, *Electroanalysis*, 2014, **26**, 1345–1353.
196 P. Kassal, J. Kim, R. Kumar, W. R. de Araujo, I. M. Steinberg, M. D. Steinberg and J. Wang, *Electrochem. Commun.*, 2015, **56**, 6–10.
197 X. Liu and P. B. Lillehoj, *Biosens. Bioelectron.*, 2017, **98**, 189–194.
198 X. Liu and P. B. Lillehoj, *Proc. Micro Electro Mech. Syst.*, 2017, 377–380.
199 P. Mostafalu, W. Lenk, M. R. Dokmeci, B. Ziaie, A. Khademhosseini and S. R. Sonkusale, *IEEE Trans. Biomed. Circuits Syst.*, 2015, **9**, 670–677.
200 M. F. Farooqui and A. Shamim, *Sci. Rep.*, 2016, **6**, 28949.
201 B. Melai, P. Salvo, N. Calisi, L. Moni, A. Bonini, C. Paoletti, T. Lomonaco, V. Mollica, R. Fuoco and F. Di Francesco, *Proc. IEEE Eng. Med. Biol. Soc., IEEE Int. Conf., 38th*, 2016, pp. 1898–1901.
202 D. A. Jankowska, M. B. Bannwarth, C. Schulenburg, G. Faccio, K. Maniura-Weber, R. M. Rossi, L. Scherer, M. Richter and L. F. Boesel, *Biosens. Bioelectron.*, 2017, **87**, 312–319.
203 M. K. Nakhleh, H. Amal, R. Jeries, Y. Y. Broza, M. Aboud, A. Gharra, H. Ivgi, S. Khatib, S. Badarneh, L. Har-Shai, L. Glass-Marmor, I. Lejbkowicz, A. Miller, S. Badarny, R. Winer, J. Finberg, S. Cohen-Kaminsky, F. Perros, D. Montani, B. Girerd, G. Garcia, G. Simonneau, F. Nakhoul, S. Baram, R. Salim, M. Hakim, M. Gruber, O. Ronen, T. Marshak, I. Doweck, O. Nativ, Z. Bahouth, D. Shi, W. Zhang, Q. Hua, Y. Pan, L. Tao, H. Liu, A. Karban, E. Koifman, T. Rainis, R. Skapars, A. Sivins, G. Ancans, I. Liepniece-Karele, I. Kikuste, I. Lasina, I. Tolmanis, D. Johnson, S. Z. Millstone, J. Fulton, J. W. Wells, L. H. Wilf, M. Humbert, M. Leja, N. Peled and H. Haick, *ACS Nano*, 2017, **11**, 112–125.
204 T. H. Risby and S. F. Solga, *Appl. Phys. B: Lasers Opt.*, 2006, **85**, 421–426.
205 M. J. Maisels and E. Kring, *Pediatrics*, 2006, **118**, 276–279.
206 T. Hibbard and A. J. Killard, *Crit. Rev. Anal. Chem.*, 2011, **41**, 21–35.
207 M. G. Persson, L. E. Gustafsson, O. Zetterström, V. Agrenius and E. Ihre, *Lancet*, 1994, **343**, 146–147.
208 C. N. Tassopoulos, D. Barnett and T. Russell Fraser, *Lancet*, 1969, **293**, 1282–1286.
209 J. Hodgkinson and R. P. Tatam, *Meas. Sci. Technol.*, 2013, **24**, 012004.
210 K.-H. Kim, S. A. Jahan and E. Kabir, *TrAC, Trends Anal. Chem.*, 2012, **33**, 1–8.
211 J. M. Corres, I. R. Matias, M. Hernaez, J. Bravo and F. J. Arregui, *IEEE Sens. J.*, 2008, **8**, 281–285.
212 M. Righettoni, A. Tricoli, S. Gass, A. Schmid, A. Amann and S. E. Pratsinis, *Anal. Chim. Acta*, 2012, **738**, 69–75.
213 S. Borini, R. White, D. Wei, M. Astley, S. Haque, E. Spigone, N. Harris, J. Kivioja and T. Ryhänen, *ACS Nano*, 2013, **7**, 11166–11173.
214 M. C. Caccami, M. Y. S. Mulla, C. D. Natale and G. Marrocco, *Proc. 11th Eur. Conf. Antennas Propag.*, 2017, pp. 3394–3396.
215 L. Wang, J. A. Jackman, J. Hyeon Park, E.-L. Tan and N.-J. Cho, *J. Mater. Chem. B*, 2017, **5**, 4019–4024.
216 S. Ammu, V. Dua, S. R. Agnihotra, S. P. Surwade, A. Phulgirkar, S. Patel and S. K. Manohar, *J. Am. Chem. Soc.*, 2012, **134**, 4553–4556.

217 C. Di Natale, R. Paolesse, E. Martinelli and R. Capuano, *Anal. Chim. Acta*, 2014, **824**, 1–17.
218 K. Arshak, E. Moore, G. M. Lyons, J. Harris and S. Clifford, *Sens. Rev.*, 2004, **24**, 181–198.
219 J. W. Gardner, H. W. Shin and E. L. Hines, *Sens. Actuators, B*, 2000, **70**, 19–24.
220 T. Seesaard, P. Lorwongtragool and T. Kerdcharoen, *Sensors*, 2015, **15**, 1885–1902.
221 N. Kahn, O. Lavie, M. Paz, Y. Segev and H. Haick, *Nano Lett.*, 2015, **15**, 7023–7028.
222 H. Jin, T.-P. Huynh and H. Haick, *Nano Lett.*, 2016, **16**, 4194–4202.
223 P. Lorwongtragool, E. Sowade, N. Watthanawisuth, R. Baumann and T. Kerdcharoen, *Sensors*, 2014, **14**, 19700–19712.
224 S. Imani, A. J. Bandodkar, A. M. V. Mohan, R. Kumar, S. Yu, J. Wang and P. P. Mercier, *Nat. Commun.*, 2016, **7**, 11650.
225 M. Kaltenbrunner, M. S. White, E. D. Głowacki, T. Sekitani, T. Someya, N. S. Sariciftci and S. Bauer, *Nat. Commun.*, 2012, **3**, 770.
226 Y.-H. Lee, J.-S. Kim, J. Noh, I. Lee, H. J. Kim, S. Choi, J. Seo, S. Jeon, T.-S. Kim, J.-Y. Lee and J. W. Choi, *Nano Lett.*, 2013, **13**, 5753–5761.
227 X. Pu, L. Li, H. Song, C. Du, Z. Zhao, C. Jiang, G. Cao, W. Hu and Z. L. Wang, *Adv. Mater.*, 2015, **27**, 2472–2478.
228 V. G. H. Eijsink, A. Bjørk, S. Gåseidnes, R. Sirevåg, B. Synstad, B. van den Burg and G. Vriend, *J. Biotechnol.*, 2004, **113**, 105–120.
229 A. J. Bandodkar, W. Jia, J. Ramírez and J. Wang, *Adv. Healthcare Mater.*, 2015, **4**, 1215–1224.
230 C. Mateo, J. M. Palomo, G. Fernandez-Lorente, J. M. Guisan and R. Fernandez-Lafuente, *Enzyme Microb. Technol.*, 2007, **40**, 1451–1463.
231 A. Pantelopoulos and N. G. Bourbakis, *IEEE Trans. Syst., Man, Cybern., Syst., Part C: Appl. Rev.*, 2010, **40**, 1–12.